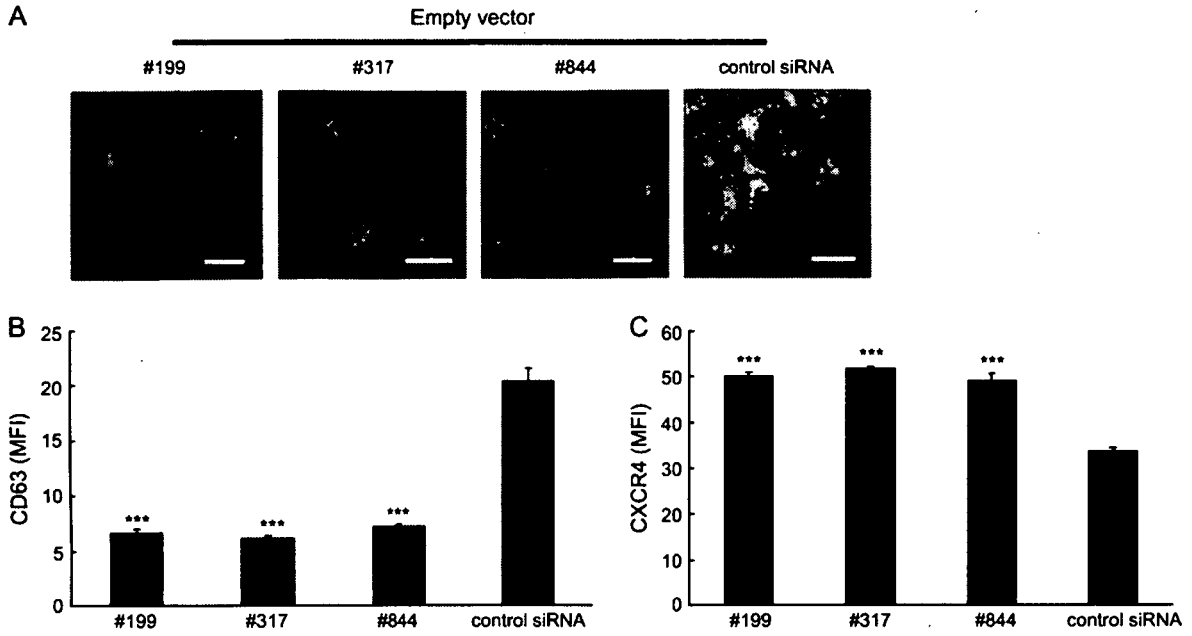

Figure 3: Suppression of CXCR4 surface expression by endogenous CD63. (A) Efficient depletion of endogenous CD63. Empty vector-transduced MAGIC-5 cells were transfected with siRNA oligonucleotides against *cd63* or control siRNA, then stained with an anti-CD63 mAb, and analyzed by confocal microscopy. Images were acquired through band-pass filters (BPF) 500–520 nm (CD63: green) and BPF 420-470 nm (Hoechst: blue). Scale bar, 30 μm. (B, C) Significant reduction of CD63 and augmentation of CXCR4 surface expression on *cd63*-depleted MAGIC-5 cells. CD63 (B) or CXCR4 (C) expression on empty vector-transduced cells treated with siRNA oligonucleotides against *cd63* was measured by flow cytometry. Data are represented as mean SED, n 3, $^{***}P < 0.05$ (vs. control siRNA).

(ii) disappearance of CXCR4 protein because of its rapid degradation; or (iii) mislocalization of CXCR4 protein.

Firstly, we compared the amounts of CXCR4 protein in untransduced cells and cells transduced with CD63ΔN or empty vector. Western blotting analysis indicated that the total amounts of CXCR4 protein were very similar in these cells (Figure 4A), suggesting that possibility (i) can be eliminated.

Next, we compared the rate of CXCR4 degradation in empty vector- and CD63ΔN-transduced cells. From examination of CXCR4 expression in cells transfected with pHA-CXCR4 after cycloheximide (CHX) treatment, an inhibitor of translation, we found that the degradation rate of CXCR4 was very similar between empty vector- and CD63ΔN-transduced MAGIC-5 cells (Figure 4B). Under the same condition, we found that little CD63ΔN degradation occurred (data not shown). These data suggest that possibility (ii) can be eliminated.

From immunofluorescent staining, we found that there was a large amount of intracellular CXCR4 in CD63ΔN-transduced cells, while the majority of CXCR4 localized at the plasma membrane in untransduced or empty vector-transduced cells (Figure 4C). To confirm this phenomenon, we next transfected an hrGFP-tagged CXCR4 DNA (phrGFPCXCR4) into empty vector- or CD63ΔN-transduced MAGIC-5 cells. This enabled us to visualize the location of CXCR4 molecules in live cells. CXCR4 was predominantly

Figure 2: Suppression of CXCR4 surface expression by CD63 or CD63 mutants. A–C) The surface expression of CXCR4 (A), CD25 (B) or CD71 (C) on CD63wt- or CD63 mutant-transduced MT-4 cells was measured by flow cytometry. The *x*-axis indicates MOI of lentiviral vector and *y*-axis indicates the mean fluorescence intensity (MFI). A-80 mAb was used for CXCR4-staining. D) Surface expression of CXCR4, CCR5, CD4 or CD71 on CD63ΔN-transduced MAGIC-5 cells was measured by flow cytometry. The number in each panel indicates the MFI of each molecule. E) The disappearance of CXCR4 on the cell surface of CD63ΔN-transduced MAGIC-5 cells. Empty vector- or CD63ΔN-transduced cells were incubated with another anti-CXCR4 mAb (A-145) at 4°C without permeabilization and analyzed by confocal microscopy. Images were acquired through band-pass filters (BPF) 500–520 nm (CXCR4: green) and BPF 420–470 nm (Hoechst: blue). Scale bars, 20 μm. F) Surface expression of CXCR4 on the CD63ΔN-transduced human CD4 T cells derived from PBMC. Six days after transduction, cells were stained with an anti-CXCR4 mAb (A-80) and analyzed. MFI of CXCR4 is shown. Data are represented as mean SED, n 4, $^{***}P < 0.05$ (vs. empty vector). G) Chemotactic response of MAGIC-5 cells to SDF-1 was reduced by transduction of CD63ΔN. Cells were cultured in the presence (black filled) or absence (grey filled) of SDF-1. Chemokine-mediated migration of cells is expressed as the mean number of migrated cells per three examined fields. Data are represented as mean SED, n 3, $^{***}P < 0.05$, NS, not significant.

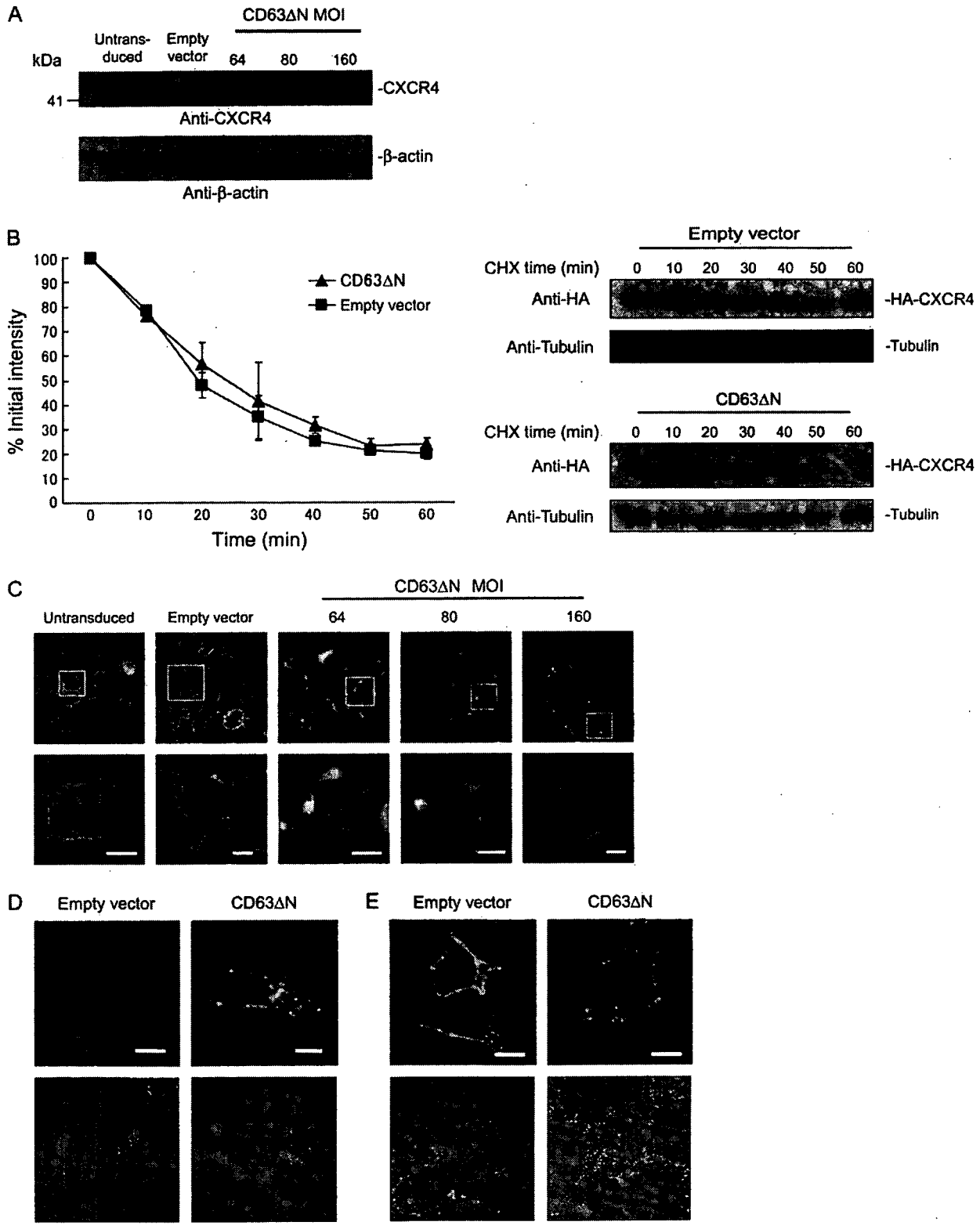

Figure 4: Legend on next page.

localized at the plasma membrane in empty vector-transduced cells, while large amounts of intracellular CXCR4 was found in CD63ΔN-transduced cells (Figure 4D). Intracellular CXCR4 was also found in 293T cells co-transfected with CD63ΔN DNA and phrGFPCXCR4 (Figure 4E). These data strongly suggest that CD63ΔN induces the mislocalization of CXCR4, in which localization of CXCR4 was shifted from the plasma membrane to intracellular membrane.

The mislocalization of CXCR4 might not be due to dynamin-dependent internalization

To clarify the mechanism of this mislocalization, we hypothesized that in CD63ΔN-transduced cells, (i) endocytosis of CXCR4 from the cell surface is strongly augmented; (ii) the intracellular trafficking of CXCR4 via vesicular transport is inhibited or (iii) CXCR4 is transported only to intracellular organelles. To examine CXCR4 surface expression on live cells over a set period of time, we cultured empty vector- or CD63ΔN-transduced MAGIC-5 cells in the presence of an fluorescein isothiocyanate (FITC)-conjugated anti-CXCR4 mAb and then assessed CXCR4 surface expression using confocal microscopy (Figure 5A). Thirty minutes after initiation of culture, CXCR4 was detected on the plasma membrane of empty vector-transduced cells (Figure 5A,c) but not visible on CD63ΔN-transduced cells (Figure 5A,e). Small green spots, probably unspecifically endocytosed or pinocytosed mAb, were also detected not only in cells cultured with anti-CXCR4 mAbs (Figure 5A,c.e) but also in cells cultured with an FITC-conjugated control immunoglobulin (Ig) G (Figure 5A,a). We next carried out the similar experiment in the presence of an actin polymerization inhibitor, cytochalasin D, and confirmed that there was little captured control IgG (Figure 5A,g). In this condition, CXCR4 on the plasma membrane was detected only in empty vector-transduced cells (Figure 5A,i), but not visible in CD63ΔN-transduced cells (Figure 5A,k). CXCR4 on the cell surface was not detected in CD63ΔN-transduced cells after further incubation (120 min) (Figure 5A,o). In addition, we transfected a dominant negative mutant of dynamin 1 (Dynamin 1 K44A) DNA into CD63ΔN-transduced MAGIC-5 cells to block dynamin-dependent CXCR4 internalization (7,8). Although we found the accumulation of transferrin receptor (CD71) on the cells after transfection with Dynamin 1 K44A DNA, we could not observe any recovery of CXCR4 surface expression in the cells (Figure 5B). These data suggest that the CD63ΔN-induced CXCR4 mislocalization might not be the result of dynamin-dependent internalization.

Intracellular trafficking of CXCR4 via transport vesicles is not inhibited in CD63ΔN-transduced cells

To examine the longitudinal distribution of CXCR4 molecules in live cells, we prepared a haloalkane dehalogenase-tagged (Halo-tagged) CXCR4 DNA (pHalo-CXCR4) and transfected it into empty vector- or CD63ΔN-transduced MAGIC-5 cells. After staining with HaloTag™-specific labeling ligand (Halo-ligand), we found that CXCR4 was localized predominantly at the plasma membrane and partly in the intracellular compartment including ceramide Golgi apparatus of empty vector-transduced cells (Figure 6A, upper left panel). The labeled CXCR4 at the plasma membrane was rapidly internalized after SDF-1 stimulation (data not shown), indicating that Halo-tagged CXCR4 represents natural CXCR4 distribution. In CD63ΔN-transduced cells, however, we detected most CXCR4 in the intracellular membrane containing the ceramide Golgi apparatus, but not at the plasma membrane (Figure 6A, upper center panel). In addition, we observed many vesicle-like CXCR4 ceramide$^-$ spots in the cytoplasm of these cells (arrow heads in Figure 6A upper center panel). To confirm rigidly that the signal of these spots reflected the existence of Halo-tagged CXCR4, we treated transfected cells with Brefeldin A (BFA), an inhibitor of vesicle transport from the ER to the Golgi apparatus. We detected only reticulated distribution of CXCR4 but no vesicle-like spots in the treated cells (Figure 6A, right panel), confirming that these spots were CXCR4-containing vesicles. The longitudinal distribution of CXCR4 was next traced over 30-min time intervals (Figure 6B,C). Although we detected many CXCR4-containing vesicles during observation (arrow heads in Figure 6C), no CXCR4 at the plasma membrane was found in CD63ΔN-transduced cells. To further examine CXCR4-containing vesicles in detail, we performed analyses using total internal reflection fluorescence microscopy (TIRFM). This microscopy is adequate to trace vesicles within approximately 150 nm of the plasma membrane (adhered surface). We transfected CXCR4EGFP into empty vector- or CD63ΔN-transduced MAGIC-5 cells and successfully detected many CXCR4-containing vesicles (Figure 6D,E, upper left panels). We found a similar

Figure 4: Induction of CXCR4 mislocalization by CD63ΔN. A) Total CXCR4 expression is similar independent of CD63ΔN-transduction in MAGIC-5 cells. The total amounts of CXCR4 protein in empty vector- or CD63ΔN-transduced cells was measured by Western blotting using an anti-CXCR4 mAb (A-145). β-actin serves as a control. B) The degradation rate of HA-tagged CXCR4 in empty vector- or CD63ΔN-transduced MAGIC-5 cells. The degradation of CXCR4 in the presence of CHX was assessed by Western blotting. The decay graph shows average of three independent trials (right panel). The images of one representative blot are also shown. Tubulin serves as a control. C) Intracellular CXCR4 was found in CD63ΔN-transduced MAGIC-5 cells. Cells were stained with an anti-CXCR4 mAb (A-145), and analyzed by confocal microscopy. Images were acquired through BPF 500–520 nm (CXCR4: green) and BPF 420–470 nm (Hoechst: blue). Scale bars, 10 μm. D, E) Intracellular CXCR4 was detected in the presence of CD63ΔN. Empty vector- or CD63ΔN-transduced MAGIC-5 cells transfected with phrGFPCXCR4 (D), and 293T cells co-transfected with phrGFPCXCR4 and empty vector or CD63ΔN DNA (E), were analyzed by confocal microscopy. Images were acquired through band-pass filters (BPF) 500–520 nm (GFP: green) and BPF 420–470 nm (Hoechst: blue). Scale bars, 10 μm. DIC images are also shown (lower panel).

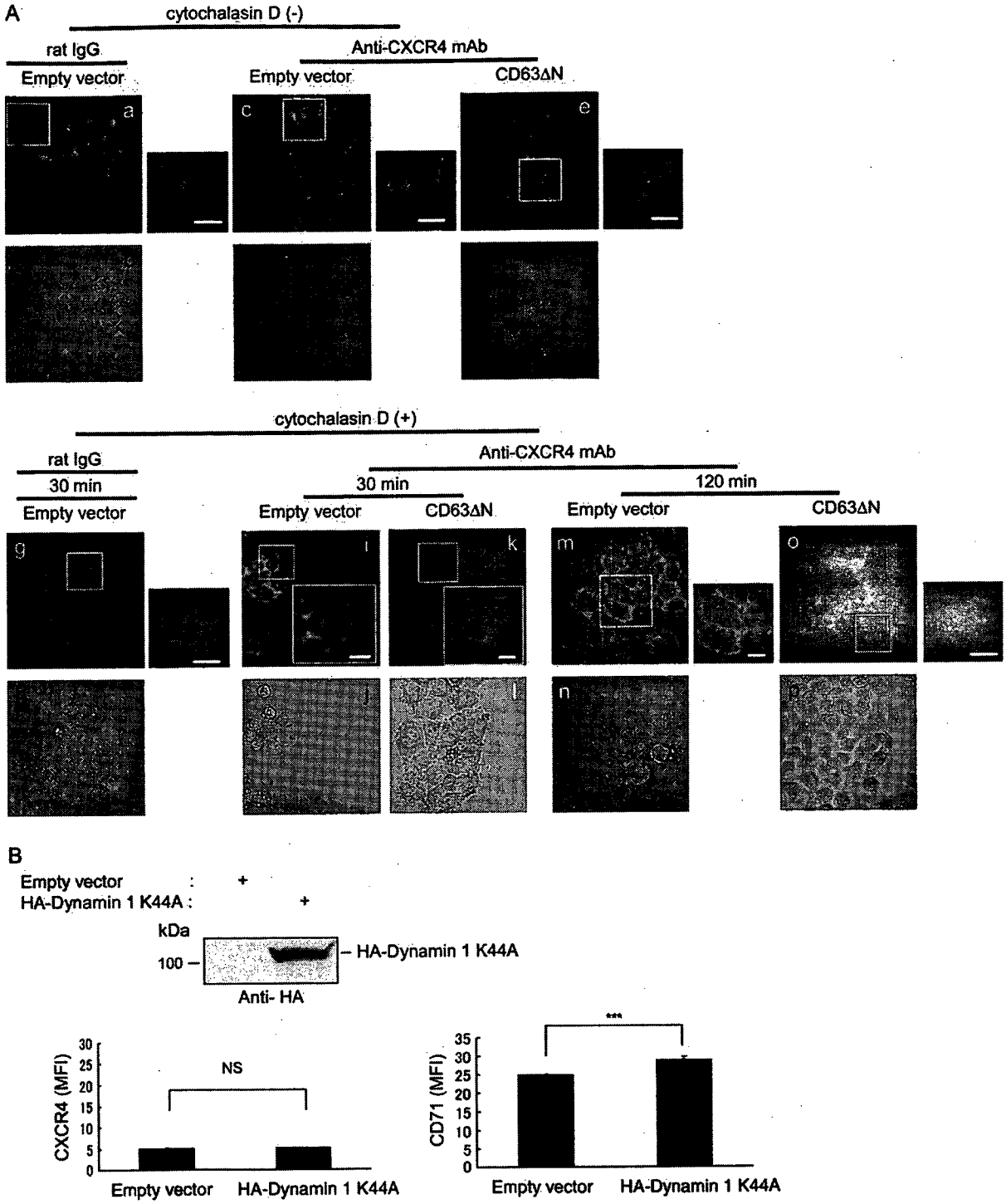

Figure 5: Absence of CXCR4 from cell surface might not be because of dynamin-dependent internalization. A) No detectable CXCR4 surface expression on CD63ΔN-transduced MAGIC-5 cells. Empty vector- and CD63ΔN-transduced cells were cultured in the presence of an FITC-labeled anti-CXCR4 mAb (A-145) for 30 min (a–f) and then analyzed by confocal microscopy. Cells supplemented with cytochalasin D (5 μM) were also cultured for 30 min (g–l) or 120 min (m–p). Enlarged images are shown in white boxes. Images were acquired through BPF 500–520 nm (CXCR4: green). Scale bars, 10 μm. DIC images are also shown (lower panel). B) CD71 but not CXCR4 surface expression was increased by dominant negative mutant of dynamin 1-transfection. CD63ΔN-transduced MAGIC-5 cells were transfected with HA-tagged Dynamin 1 K44A DNA. The expression of HA-tagged protein was confirmed by Western blotting (upper panel), and CXCR4 (lower left panel) or CD71 (lower right panel) surface expression was measured by flow cytometry. MFI of CXCR4 or CD71 was shown. Data are represented as mean SED, n 4, $***P < 0.05$, NS, not significant.

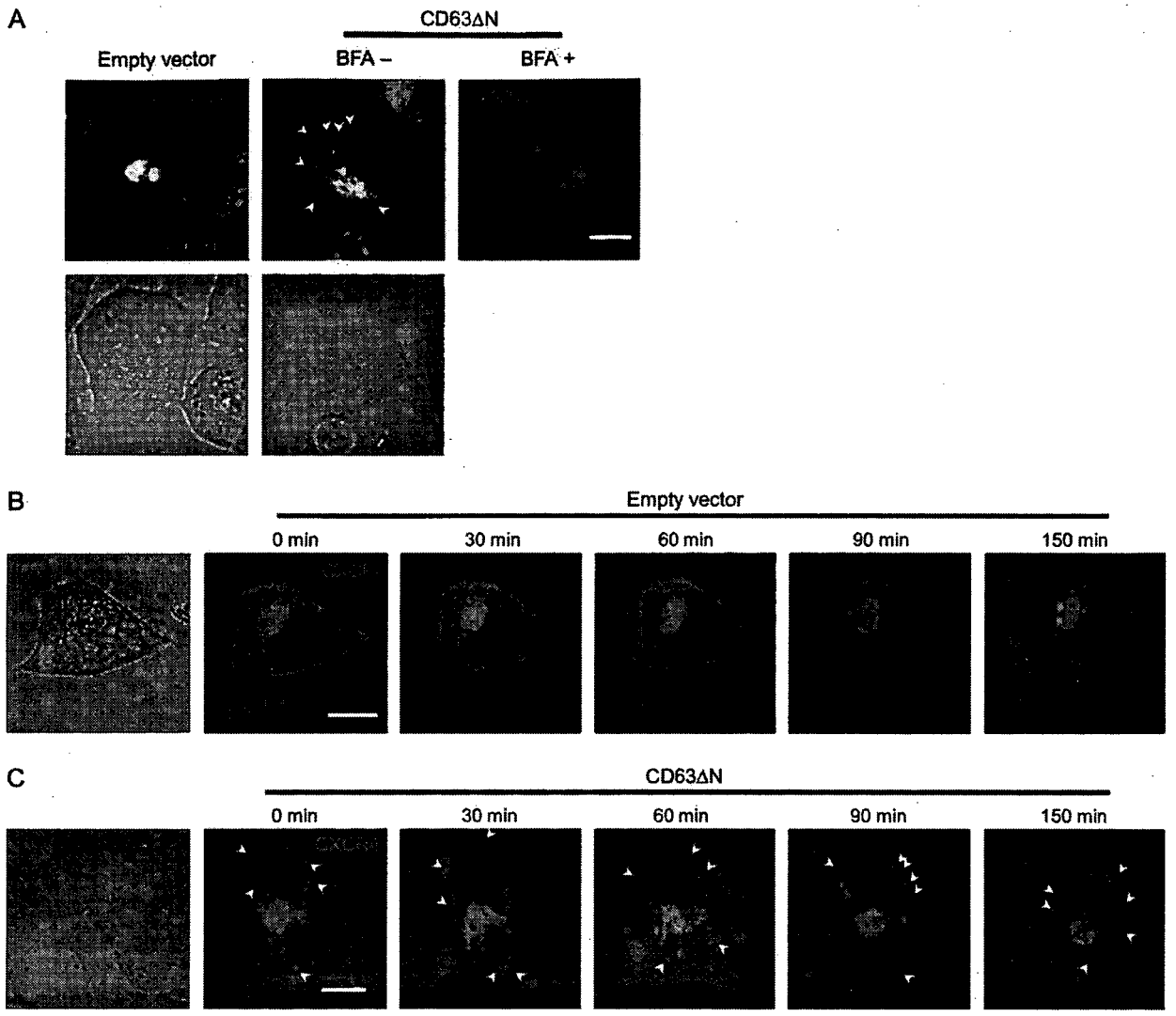

Figure 6: Intracellular trafficking of CXCR4 via transport vesicles is not inhibited. A) Localization of CXCR4 in live cells. MAGIC-5 cells were transfected with pHalo-CXCR4, stained with the Halo-ligand and ceramide (Golgi apparatus) and analyzed by confocal microscopy. Right panel shows cells cultured in medium containing 50 μg/mL of BFA without ceramide-staining. Images were acquired through band-pass filters (BPF) 500–520 nm (ceramide: green) and BPF 570–610 nm (CXCR4: magenta). Arrow heads indicate CXCR4-containing vesicles. Scale bars, 10 μm. DIC images are also shown (lower panel). B, C) Longitudinal analyses on the distribution of CXCR4. Cells were followed with confocal microscopy at the indicated time after initiation of the trace. Empty vector-transduced (B) and CD63ΔN-transduced (C) MAGIC-5 cells were studied. Arrow heads in (C) indicate CXCR4-containing vesicles in CD63ΔN-transduced cells. Scale bars, 10 μm. DIC images are also shown (first panels in B, C). D, E) empty vector-transduced (D) or CD63ΔN- transduced (E) MAGIC-5 cells were transfected with CXCR4EGFP and analyzed using TIRFM. DIC images are shown (upper right panels in D and E). Enlarged images from upper left panels in D and E (box) taken at 1-second interval are shown in middle and lower panels. Fusion-like processes between the vesicle and the plasma membrane was detected in empty vector-transduced but not in CD63ΔN-transduced cells. Arrows in middle panels in (E) indicate fusion-like process between a vesicle and the plasma membrane. Images were acquired through BPF 509–547 nm (GFP). Dotted lines indicate the plasma membrane. Scale bars, 10 μm (upper panel) and 1.7 μm (lower panel). sec, second. Figure 6 continued on next page.

number of the vesicles in both empty vector- and CD63ΔN-transduced cells (Table 1). These data suggest that the CD63ΔN-induced CXCR4 mislocalization is not because of inhibition of CXCR4 trafficking via transport vesicles. CXCR4 is suggested to be transported to intracellular organelles, but not to the plasma membrane. As precise quantification of fusion to the plasma membrane was difficult in this assay, we were not able to quantify the fusion events. Interestingly, however, we could capture some fusion-like processes between CXCR4-containing vesicles and the plasma membrane in empty vector-transduced cells (one of them was shown in Figure 6D, arrows in middle panels) but not in CD63ΔN-transduced cells (Figure 6E).

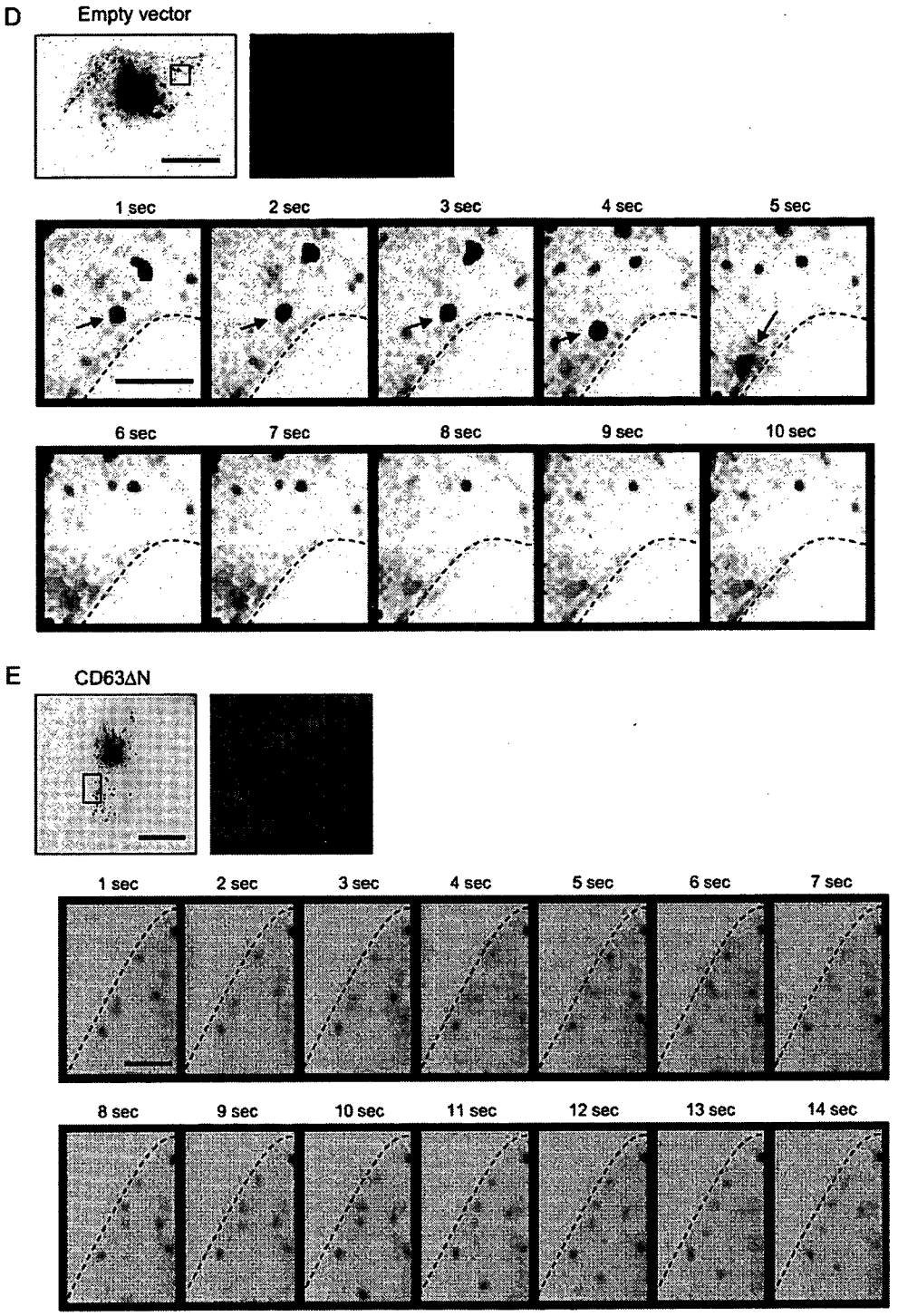

Figure 6: Continued from previous page.

Mislocalized CXCR4 appears to be destined in the late endosomes/lysosomes

To investigate the mislocalization of CXCR4 further, we carried out a series of immunofluorescent staining using antibodies against marker molecules in several different organelles. Figure 7A shows that the intracellular CXCR4 in CD63ΔN-transduced cells were predominantly located in the *cis*-Golgi (Golgi matrix protein of 130 kDa: GM130), the TGN (p230) and the late endosomes/lysosomes (LAMP-1), but not in the early endosomes (early endosome antigen 1,

Table 1: Quantification of CXCR4-containing vesicles[a]

	Counted cells	Total	Average (per a cell[b])
Empty vector	9	1144	127.1
CD63ΔN	19	2257	118.8

[a]Number of vesicles was counted by BASIC METAMORPH software.
[b]Number of vesicles was divided by numbers of cells.

EEA1). It was also partly located in the ER (calnexin) and the vesicles and tubular clusters (ERGIC-53). We also found that a large fraction of intracellular CXCR4 co-localized with lysosome marker, a low internal pH indicator; LysoTracker in CD63ΔN-transduced MAGIC-5 cells transfected with phrGFPCXCR4 (Figure 7A, right panels). The ratio of the merged area where CXCR4 localized with each intracellular organelle is shown in Figure 7B. This graph shows that no CXCR4 is retained in any specific organelle and that the CXCR4 appears to be transported to the late endosomes/lysosomes. By contrast, in empty vector-transduced cells, CXCR4 was mainly found at the plasma membrane and additionally in the ER (Figure S2). We next assessed whether or not CXCR4 is destined to the lysosome-dependent degradation in CD63ΔN-transduced cells using lysosomal inhibitors (chloroquine, CHQ or concanamycin A, CMA) (Figure 7C). In the inhibitor-treated cells, CXCR4 degradation after CHX treatment was clearly inhibited, indicating that most CXCR4 was transported to lysosomes and subsequently degraded in CD63ΔN-transduced cells.

CD63ΔN co-localizes and interacts with CXCR4

To investigate the intracellular co-localization of CD63ΔN and CXCR4, we prepared a FLAG-tagged CD63ΔN (FLAGCD63ΔN)-expressing lentiviral vector and confirmed that its ability to suppress CXCR4 surface expression was similar to that of untagged vector (data not shown). Then, we examined the co-localization of CD63ΔN and CXCR4 in FLAGCD63ΔN-transduced MAGIC-5 cells using confocal microscopy. As shown in Figure 8A, CD63ΔN molecules mainly overlapped with CXCR4 in the perinuclear region. Similar co-localization of CD63ΔN and CXCR4 was also reproduced in 293T cells co-transfected with phrGFPCXCR4 and a red fluorescent protein–tagged CD63ΔN DNA (DsRed-CD63ΔN) (data not shown). Further immunofluorescent staining experiments using antibodies against organelles marker molecules indicated that CD63ΔN was mainly localized in the late endosomes and the TGN (Figure 8B). To gain insight into the relationship between CD63ΔN and CXCR4, we next examined intracellular interaction between these molecules. In addition to CD63ΔN, CD63wt was also examined. As shown in right panel of Figure 8C, CD63ΔN and CD63wt co-precipitated with CXCR4 in 293T cells co-transfected with hemagglutinin (HA)-tagged CXCR4 DNA (pHA-CXCR4) and a FLAG-tagged CD63ΔN or CD63wt DNA. The affinity of CD63ΔN to CXCR4 appeared to be higher than that of CD63wt. CD63wt but not CD63ΔN had an ability to interact with MT1-MMP as reported previously (20).

Requirement of a CXCR4 C-terminal cytoplasmic tail for CD63ΔN-induced suppression in CXCR4 surface expression

To explore the responsible region of CXCR4 for the CD63ΔN-induced suppression, we used a series of EGFP-tagged CXCR4 C-terminal cytoplasmic tail-deletion mutant DNA (C-terminal tail; 14 amino acids from C-termini) (26) (Figure 9A) and transfected them into empty vector- or CD63ΔN-transduced MAGIC-5 cells. Having confirmed that these mutants were expressed on the cell surface of empty vector-transduced cells (data not shown), we measured CXCR4 mutant surface expression on CD63ΔN-transduced cells using flow cytometry. Interestingly, we found that CXCR4 surface expression was sustained in cells transfected with a mutant lacking six amino acids in the C-terminal tail (Figure 9B). The distribution of CXCR4EGFP or these mutants in CD63ΔN-transduced MAGIC-5 cells is also shown in Figure 9C. These mutants but not CXCR4EGFP (wild type) were localized at the plasma membrane. From these data, we deduced that this six amino acid-deletion provided resistance to the CD63ΔN-induced suppression of CXCR4 surface expression. We observed a similar phenomenon in 293T cells co-transfected with CD63ΔN and EGFP-tagged CXCR4-deletion mutant DNA (data not shown). These results indicate that the C-terminal six amino acids (^{347}SSFHSS^{352}) are involved in the CD63ΔN-induced suppression of CXCR4.

Discussion

In this study, we successfully identified a mutant of a tetraspanin protein (CD63ΔN) as an inhibitor of X4 HIV-1-induced CPE by our screening strategy using a novel cDNA library-expressing lentiviral vector system (2). Then, we showed that CD63ΔN inhibited X4 HIV-1 infection (Figure 1E,G). The inhibition was observed in X4 HIV-1 but not in MLV-pseudotyped HIV-1 (Figure 1F) or R5 HIV-1 (Figure 1G). Because the difference between X4 HIV-1 and R5 HIV-1 lies upon co-receptor usage at the viral entry, we predicted and confirmed that CD63ΔN induced the suppression of CXCR4 surface expression (Figure 2A,D). These data provide the evidence that localization of co-receptor molecules at the plasma membrane is crucial for HIV-1 entry and by depleting the surface expression of co-receptor proteins, HIV-1 target cells can effectively escape from its infection.

It has been shown that anti-CD63 Ab (27) or recombinant soluble CD63-EC2 proteins (28) inhibited HIV infection in macrophages without affecting expression of CD4 or co-receptor. However, we clearly showed that a CD63 N-terminal deletion mutant blocks X4 HIV-1 entry via specific suppression of CXCR4 surface expression on target cells (Figure 2A,D,E–G). It has not been yet reported that CD63 or its mutants induce downregulation of CXCR4.

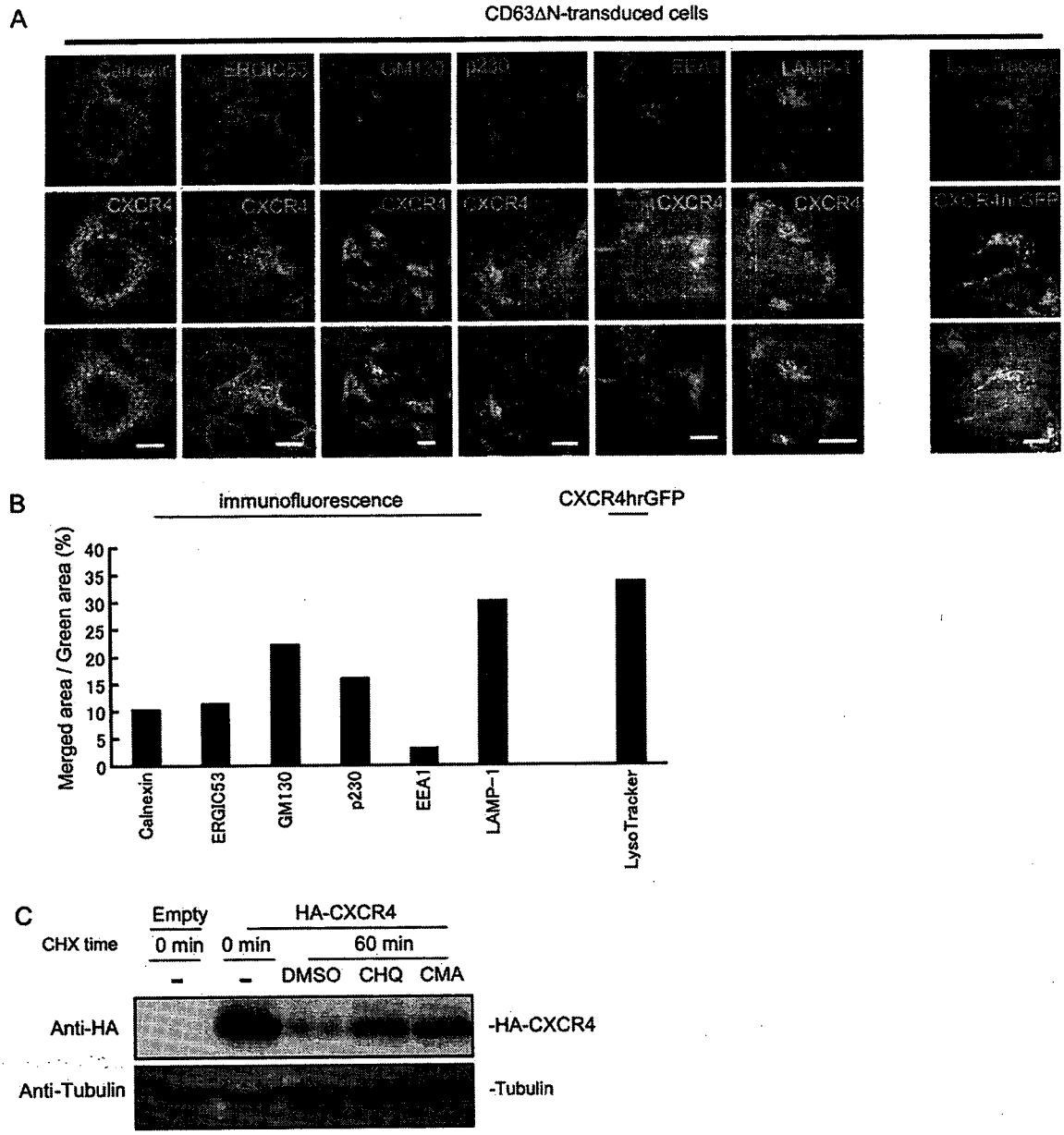

Figure 7: CXCR4 was transported only toward intracellular organelles. A) Co-localization of CXCR4 with intracellular organelles in CD63ΔN-transduced MAGIC-5 cells. Images were acquired through band-pass filters (BPF) 500–520 nm (CXCR4 and CXCR4hrGFP: green), BPF 650–700 nm (intracellular organelles: magenta) and BPF 420–450 nm (LysoTracker: magenta). Merged images are shown in bottom. Scale bars, 10 μm. Calnexin: ER; ERGIC53: Vesicular-tubular transport complex (VTCs); GM130: *cis*-Golgi; p230: TGN; EEA1: early endosomes; and LAMP-1: late endosomes. B) The ratio of merged area where CXCR4 co-localized with each intracellular organelle in (A) (merged area/CXCR4 area) was shown. C) The lysosome-dependent degradation of HA-tagged CXCR4 in CD63ΔN-transduced MAGIC-5 cells. The degradation of CXCR4 in the presence of CHX with two classes of lysosomal inhibitors, CHQ (50 μg/mL), CMA (20 μg/mL) or vehicle (DMSO), was assessed by Western blotting. Tubulin served as a control. The results of one of three, independently conducted, experiments are shown.

Although these previous findings and our presented phenomena seem to occur by distinct mechanisms, it might be true that CD63 has some functions in HIV infection.

By flow cytometric analyses, we confirmed the CD63ΔN-induced CXCR4 downregulation in MT-4 (Figure 2A), MAGIC-5 (Figure 2D) and 293T cells (data not shown) as well as human primary CD4 T cells (Figure 2F), natural target cells for HIV-1. These data suggest that this CD63ΔN-induced suppression is not a cell type-dependent phenomenon. The significant but lower suppression of CXCR4 in CD4 T cells (Figure 2F) can be explained by the lower efficiency of lentiviral transduction. Also, primary CD4 T cells needed to be activated with immobilized

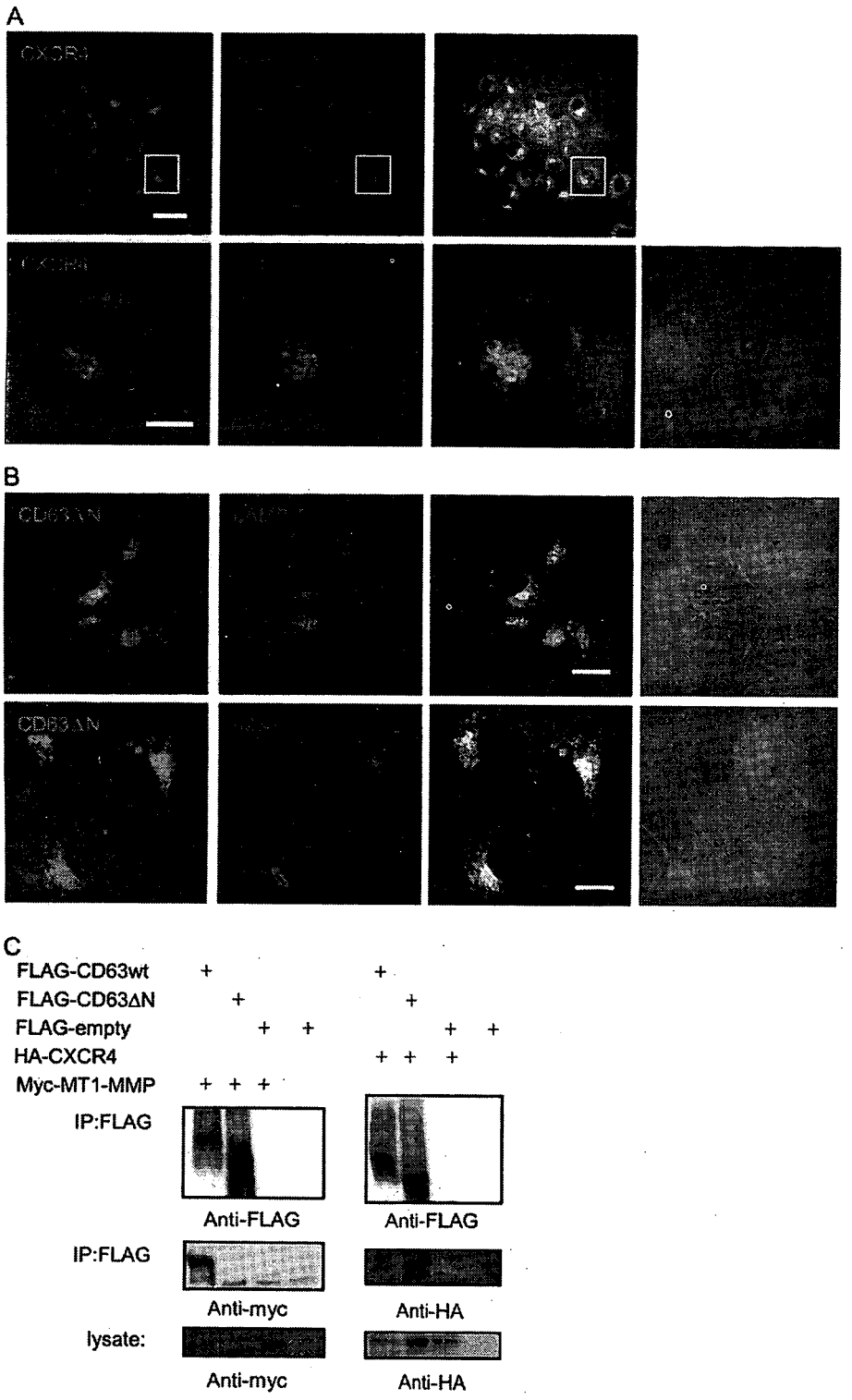

Figure 8: Co-distribution and interaction of CD63ΔN with CXCR4. A) Localization of CXCR4 and CD63ΔN. FLAGCD63ΔN-transduced MAGIC-5 cells were stained with an anti-CXCR4 mAb and an anti-FLAG pAb. Images were acquired through band-pass filters (BPF) 500–520 nm (CXCR4: green) and BPF 650–700 nm (FLAG: magenta) and merged images are shown. Scale bars, 50 μm (upper panels) and 10 μm (lower panels). B) Co-localization of FLAGCD63ΔN with intracellular organelles in FLAGCD63ΔN-transduced MAGIC-5 cells. Images were acquired through BPF 500–520 nm (FLAG: green) and BPF 650–700 nm (intracellular organelles: magenta). Merged images are shown in third panels. Scale bars, 10 μm. LAMP-1, late endosomes; and p230: TGN. C) Molecular interaction between CXCR4 and CD63ΔN or CD63wt. FLAG-tagged CD63ΔN or CD63wt were immunoprecipitated (IP) with an anti-FLAG mAbs and immunoblotted with an anti-HA and an anti-FLAG mAb (right panel). Lysate were also subjected to Western blot to detect expression of HA-tagged CXCR4. Interaction between CD63wt and MT1-MMP was shown as a control (left panel). The results of one of three, independently conducted, experiments are shown.

anti-CD3/CD28 mAbs during lentiviral transduction. As CXCR4 surface expression is reduced on activated CD4 T cells (29), primary CD4 T cells had lower expression of CXCR4 compared with that of cell lines to start with. In addition to flow cytometric analyses, we confirmed the CXCR4 downregulation by immunofluorescent analysis without permeabilization (Figure 2E) and the reduced response to SDF-1 by CD63ΔN-transduced cells (Figure 2G).

CD63 is known to form TEMs on the plasma membrane with other tetraspanin proteins (11). Do TEMs play any role

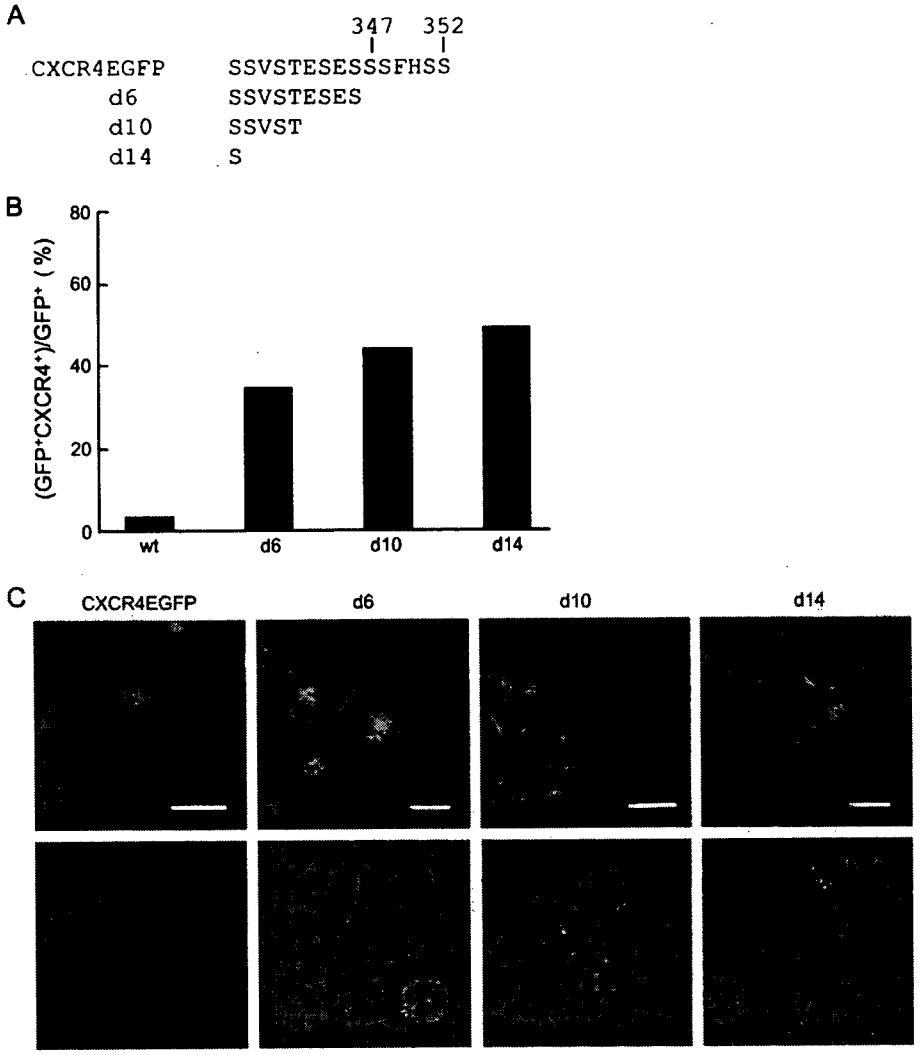

Figure 9: Requirement of CXCR4 C-terminal cytoplasmic tail for CD63ΔN-induced suppression in CXCR4 surface expression. A) Amino acid sequence of the C-terminal tail of CXCR4. Shown is the amino acid sequence (single-letter code) of the C-terminal tail of wild-type CXCR4, along with the various mutants used in this experiment. B) Sustainment of CXCR4 surface expression from its C-terminal tail-deletion mutant in CD63ΔN-transduced cells. CD63ΔN-transduced MAGIC-5 cells were transfected with CXCR4EGFP, or its C-terminal tail-deletion mutants (d6, d10 or d14), and CXCR4 surface expression and GFP were measured by flow cytometry. Percentage of GFP CXCR4 cells out of total GFP cells is shown. Results of one of three, independently conducted, experiments are shown. C) Expression at the plasma membrane was detected for d6, d10 or d14 mutants but not for CXCR4EGFP in the presence of CD63ΔN. CD63ΔN-transduced MAGIC-5 cells transfected with CXCR4EGFP or the mutant DNA, were analyzed by confocal microscopy. Images were acquired through band-pass filters 500–520 nm (GFP: green). Scale bars, 10 μm. DIC images are also shown (lower panel).

in the CD63ΔN-induced suppression? The first question was whether CD63ΔN has any effect on the surface expression of other tetraspanin proteins. The cell surface expression of other tetraspanin proteins such as CD9, CD53, CD81, CD82 and CD151 was not changed in CD63ΔN-transduced MAGIC-5 cells (data not shown) as well as that of CD4, CCR5 and CD71 (Figure 2D). This result suggests that the CD63ΔN-induced suppression might not be caused by any changes of TEMs. The second question was whether other tetraspanin proteins inhibit CXCR4 surface expression. Although CD63wt suppressed CXCR4 surface expression (Figure 2A), we found that CD9, CD81 or CD151 have no suppressive activity on CXCR4 surface expression in MT-4 cells (data not shown). These data strongly suggested that TEMs are not involved in the CD63ΔN-induced suppression. Furthermore, we also found that knockdown of endogenous CD63 resulted in increase of CXCR4 surface expression (Figure 3C). Thus, we deduced that CD63 itself possesses some suppressive ability for CXCR4 surface expression, probably in a TEMs-independent manner.

We next showed that the CD63ΔN-induced disappearance of surface CXCR4 is not because of suppression on gene expression (Figure 4A) or rapid degradation (Figure 4B), but most likely the result of mislocalization of CXCR4. From immunofluorescent analysis and confocal microscopic analysis using phrGFPCXCR4, we found large amounts of intracellular CXCR4 in CD63ΔN-transduced cells but not at the plasma membrane (Figure 4C–E). There have been many reports on the downregulation of cell surface proteins caused by mislocalization. The downregulation of major histocompatibility complex (MHC) class I molecules from the cell surface upon viral infection may be the most well known (30). To evade the monitoring of cytotoxic T lymphocyte, some viral proteins induce mislocalization of MHC class I molecules by many strategies such as (i) rapid internalization, (ii) inhibition of egress from the ER and (iii) re-routing of MHC class I molecules. MHC class I molecules such as human leukocyte antigen (HLA)-A and -B are endocytosed by the HIV Nef and phosphofurin acidic cluster sorting protein-1 in the ARF 6 pathway (31,32). MHC class I molecules (HLA) are prevented from

being transported to the plasma membrane by the adenovirus gene product E3/19K (E19) (33). The re-routing of MHC class I molecules to the lysosome is induced by the human herpesvirus 7 glycoprotein U21 and the mouse cytomegalovirus early gene product (gp48) (34,35).

In the case of CXCR4, rapid internalization was our first guess because CD63 has been reported to play roles in endocytosis of interaction partners such as the HKβ (19) and MT1-MMP (20). Duffield et al. showed that the HKβ interacted with CD63 and the HKβ/CD63 complex was efficiently internalized. When the interaction between CD63 and AP complexes was disrupted, HKβ was not able to be internalized from the cell surface and was retained at the plasma membrane. Takino et al. showed that CD63 formed a complex with MT1-MMP and was involved in internalization, lysosomal targeting and proteolysis of MT1-MMP via LSM-dependent endocytosis (20). These reports suggest that CD63 acts as a mediator between the interaction partners and AP-2 complexes to enhance internalization of the CD63/interaction partner complex (36). In CD63ΔN-transduced cells, however, we could not detect any CXCR4 surface expression for 120 min in anti-CXCR4 mAb feeding experiments under conditions that inhibit actin polymerization (Figure 5A) and found that CD63ΔN-induced suppression of surface CXCR4 expression was not able to be rescued by the dominant negative mutant of dynamin 1 (Figure 5B). Moreover, we found that the CD63ΔN-induced inhibition of X4 HIV infection and suppression of CXCR4 surface expression were not impaired dramatically by LSM deletion (Figures 1E and 2A) and a CD63 mutant lacking LSM (CD63ΔL) still maintained suppressive activity (data not shown). Thus, these data suggest that this CXCR4 down-regulation might not be the result of dynamin-dependent or AP complex-dependent endocytosis. Furthermore, we found that in CD63ΔN-transduced cells, little intracellular CXCR4 was found in the early endosomes (Figure 7A, EEA1). As endocytosed membrane proteins are first collected in the early endosome, this data support the hypothesis that there is little CXCR4 endocytosis in CD63ΔN-transduced cells. Although role of CD63 in these previous studies and that of CD63ΔN in our study appears to be distinct, CD63 has some roles in intracellular trafficking of other proteins.

We showed that intracellular trafficking of CXCR4 via vesicular transport was not stopped by CD63ΔN transduction. The number of CXCR4-containing transport vesicles was not reduced by CD63ΔN transduction (Table 1). We showed that there is no ER retention of CXCR4 in CD63ΔN-transduced cells because the distribution of CXCR4 in CD63ΔN-transduced cells was distinct from that in cells with BFA-induced CXCR4 retention in the ER (Figure 6A). Furthermore, CXCR4 seemed to be distributed in the Golgi of CD63ΔN-transduced cells (Figure 7A,B). This is direct evidence that further rejects the hypothesis that CXCR4 is retained in ER. The fact that a large amount of CXCR4 was also found in the late endosomes/lysosome (Figure 7A,B) indicates the existence of post-Golgi transportation and brings up the possibility that transportation of CXCR4 takes place in CD63ΔN-transduced cells. If lysosome-dependent degradation of CXCR4 indeed takes place in these cells, it should be able to be inhibited by lysosomal inhibitors (CHQ or CMA) treatment. When CD63ΔN-transduced cells were treated with CHX and CHQ or CMA, the degradation of CXCR4 was greatly inhibited (Figure 7C). This biochemical assay confirms the lysosome-dependent degradation of CXCR4, and together with the immunofluorescent analysis, shows that CXCR4 is localized and destroyed in the lysosome.

In this study, we found that six amino acids (^{347}SSFHSS^{352}) in the CXCR4 C-terminal tail were crucial for the CD63ΔN-induced CXCR4 mislocalization (Figure 9B, C). Some motifs in the CXCR4 C-terminal region such as di-leucine motif (^{328}IL^{329}) (37) and the integrity of specific serine residues in the C-terminal tail (S^{324}, S^{325}, S^{338} and S^{339}) (7) have been found to be important for localization of CXCR4. However, all the currently known motifs are involved in the internalization of CXCR4.

We also showed that CD63ΔN co-localized with CXCR4 (Figure 8A) and interacted with CXCR4 (Figure 8C). To investigate the importance of this interaction, we assessed whether the resistant mutant in Figure 9 (d6) can associate with CD63ΔN. Deletion of the six amino acids failed to abrogate association with CD63ΔN (data not shown), indicating that these amino acids are not the binding motif for CD63 (CD63ΔN). However, interaction between CXCR4 and CD63ΔN may still be a part of mechanism of changes in CXCR4 trafficking. There may be subtle differences in affinities of wild-type CXCR4 and d6 mutant to CD63ΔN, or CD63ΔN may take CXCR4 to another interacting protein, which binds through the C-terminal amino acids. In fact, direct molecular interaction is not necessary in the case of trafficking regulation of CD19 by another tetraspanin, CD81 (38). CD81 has been reported to have roles in transportation of CD19 to the plasma membrane (36,39,40). Moreover, a series of subsequent studies using many CD81 mutants showed that CD81 plays a variety of roles using different CD81 domains in different cellular compartments (38). CD63 might also have variety of roles in intracellular trafficking. In fact, a large amount of CD63ΔN is in the Golgi (Figure 8B), where more than 35% of total CXCR4 in CD63ΔN-transduced cells was also found (Figures 6C and 7A,B). Since it remains unknown how CXCR4 is sorted in the Golgi, further study is required to understand the mechanism that directs of CXCR4 trafficking at the Golgi apparatus.

In summary, we successfully identified a new X4 HIV-1 entry inhibitor, CD63ΔN. CD63ΔN induced suppression of CXCR4 surface expression, and this phenomenon appears to be caused by mislocalization of CXCR4. Intracellular CXCR4 was distributed not at the plasma membrane but

in intracellular organelles such as the Golgi and the late endosomes/lysosomes and it was degraded in the lysosome. In addition, from CD63-overexpression or depletion experiments, CD63 itself appears to have a role in influencing the level of CXCR4 surface expression, which may be one of its physiological functions.

Materials and Methods

Cells and transfection

Human 293T and MAGIC-5 cells (41) and MT-4 cells were maintained as previously described (2). PBMC were prepared from a HIV-1-seronegative donor, and CD4 cells were isolated using a CD4-positive isolation kit (Dynal Biotech). These cells were stimulated with CD3/CD28 T-cell expander (Dynal) and maintained in RPMI-1640 containing 10% fetal calf serum and 100 U/mL of IL-2. For transfection, Lipofectamin 2000 transfection reagent (Invitrogen), TransIT LT-1 transfection reagent (Takara) or the calcium phosphate method were used. BFA, CMA, CHX and dimethyl sulfoxide (DMSO) were purchased from Sigma and CHQ was purchased from Wako.

DNA construction

Lentiviral vector DNA, CSII-CDF-GATEWAY-IRES-H2K^k, was constructed through the replacement of *hrGFP* with *H-2K^k* (Daiichi Pure Chemicals) in pYK005C (2). *cd63* and *cd63Δ N* was cloned from the human PBL cDNA library into a CMV promoter-driven expression plasmid, pCMV-SPORT6 (Invitrogen). Human *cxcr4* was cloned into pCMV-SPORT6 or an upstream site of *hrgfp* tag in pIRES-hrGFP (Stratagene) (pCXCR4 and phrGFPCXCR4) and pCXCR4 FL GFP, d-6 GFP, d-10 GFP, d-14 GFP (26) were used. *cd63wt*, *cd63Δ N* and *cd63Δ NL*, were cloned into p3XFLAG-CMV-10 (Sigma) and FLAG-tagged *cd63Δ N* was transferred in pCMV-SPORT6. *cxcr4* was cloned into an upstream site of a *halo* tag and downstream of HA tag in pCMV-SPORT6, respectively (pHalo-CXCR4 and pHA-CXCR4). A cDNA on pCMV-SPORT6 was transferred into CSII-CDF-GATEWAY-IRES-H2K^k through BP and LR reaction on Gateway cloning system (Invitrogen). An EGFP-expression *env*-deleted HIV-1 plasmid DNA, pNL-EGFPΔenv, was constructed with a flameshift introduced at the *Nhe*I site of the *env* in pNLEGFP by blunting and religation. pcDNA3.1( ) HA-Dyn1 K44A (MBA-93) was obtained from ATCC. The nucleotide sequences of all constructs were confirmed using ABI 377 auto-sequencer.

Antibodies

The following primary unconjugated antibodies against human proteins were used: rat anti-CXCR4 mAbs (A-80, A-145) (42), a mouse anti-CD63 mAb, a goat anti-EEA1 polyclonal antibody (pAb), a mouse anti-LAMP-1 mAb (Santa Cruz Biotechnology), a mouse anti-ERGIC53 mAb (Alexis Biochemicals), a mouse anti-GM130 mAb, a mouse anti-p230 mAb (BD Transduction), a rabbit anti-calnexin pAb (Stressgen Bioreagents), a mouse anti-tubulin mAbs (Sigma) and a mouse anti-β-actin mAb (Cell Signaling Technology). A mouse mAb and a rabbit pAb against FLAG peptides, a mouse mAbs against c-Myc peptides and a horseradish peroxidase (HRP)-conjugated rat mAb against HA peptides were purchased from Sigma, Clontech and Roche, respectively. FITC-conjugated mAbs against CD25 and a phycoerythrin (PE)-conjugated mAb against CCR5 were purchased from BD Pharmingen, FITC or PE-conjugated mouse anti-mouse H-2K^k mAbs were purchased from Cedarlane and a PE-conjugated mouse mAb against CD4 and FITC-conjugated mAbs against CD71 were purchased from Dako and Immunotech, respectively. Sera from HIV-1-infected people were used for detecting HIV-1 antigens. The following second pAbs were used: an FITC-conjugated goat anti-rat IgG antibody (American Qualex), an Alexa488-conjugated goat anti-mouse IgG pAb (Molecular Probes), Cy5-conjugated donkey pAbs against rabbit IgG, mouse IgG or goat IgG, respectively, a biotin-conjugated donkey anti-rat IgG pAb (Chemicon), a biotin-conjugated goat anti-human IgG pAb (Vector Laboratories) and a HRP-conjugated anti-mouse IgG pAb (Cell Signaling). HRP- (Zymed), PerCP- (BD Bioscience) or Alexa 488- (Molecular Probes)-conjugated streptavidin was also used.

Small interfering RNA

Synthetic siRNAs directed against *cd63* (no. 199: 5′-ACAGCUUGUCCUGAGUCAGACCAUA-3′, no. 317: 5′-GCCUGCAAGGAGAACUAUUGUCUUA-3′ and no. 844: 5′-GAGUGGAAUAGUAUCCUCCAGGUUU-3′) and Stealth RNAi Negative Control Duplexes Medium GC Duplex were purchased from Invitrogen. Transfection was performed using Lipofectamine 2000.

Flow cytometric analysis

Flow cytometric analyses using cell line were performed as previously described (2). In case of T-cells staining, Fc receptor blocker (Dynal) was used. Data was collected using FACScan or FACScalibur (BD Bioscience) and analyzed using WinMDI software.

Immunoprecipitations and Western blotting

CXCR4 was detected as previously described (42). To detect FLAG-tagged protein, cells were scraped in triple detergent containing 1% Igepal (Sigma), 0.1% SDS, 0.5% sodium deoxycholate in 20 mM Tris–HCl (pH 8) – 0.15 M NaCl – protease inhibitor cocktail Complete (Roche). For samples of deglycosylation procedure, immunoprecipitation was required. After supplementation of an anti-FLAG mAb and incubation for 12 h at 4°C in the presence of protein G-sepharose (Amersham Biosciences), immunoprecipitants were treated with Glycoprotein Deglycosylation Kit (Calbiochem) according to the manufacturer's protocol. Interaction between CD63 and CXCR4 was also detected as described above except detergent buffer, instead of triple detergent, single detergent containing 1% Triton X-100 in 50 mM Tris–HCl (pH 8) – 0.15 M NaCl – protease inhibitor cocktail Complete, was used. Immunoprecipitation and immunoblotting of MT1-MMP were carried out as previously described (20). For degradation assay, cells transfected with pHA-CXCR4 were incubated in the presence of 15 μg/mL CHX with either 50 μg/mL CHQ, 20 μg/mL CMA or vehicle control (DMSO) and harvested at the indicated times. Cells were lysed with single detergent.

HIV-1 infection

Lentiviral vector and HIV-1 preparation were carried out as described previously (2). Cells transduced with the original, CD63 mutant fragments (clone 12.03 and clone 12.22) were infected with HIV-1_{NL4-3} and expression of HIV-1 antigen was examined 4 dpi using an anti-HIV-1 human serum. CD63wt or CD63 mutant-transduced cells were infected with NL-EGFP (24) at a MOI of 0.1. Three dpi, dual color flow cytometric analysis was performed. To prepare amphotropic MLV Env-pseudotyped HIV-1, 293T cells were co-transfected with pNL4-3Δenv and pJD-1 (43). Forty-eight hours later, culture supernatants were collected and used for infection. CD63ΔN-transduced cells were infected with HIV-1_{NL4-3} or HIV-1_{JR-CSF} (44) at a MOI of 2 and then the culture supernatant was harvested. The level of HIV-1 p24^{gag} antigen was measured by ELISA (ZeptoMetrix Corp.). To detect HIV-1 DNA by polymerase chain reaction (PCR), cells were harvested 1 dpi and PCR was performed with HIV *Tat/Rev*-specific primers (45). To prepare heat inactivated HIV-1 as a negative control, viruses were incubated at 65°C for 30 min.

Chemotaxis assay

Cell migration was assayed in 24-well cell culture chambers using inserts with 8 μm pore membrane (Falcon). Membranes were pre-coated with fibronectin. Buffer including 100 nM of SDF-1 (Wako) and SYTO 24 (Molecular Probes), and MAGIC-5 cells resuspended in OPTI-MEM reduced-serum medium (Gibco) were applied on lower well and upper wells, respectively. After incubation for 12 h, cells on lower surface of the membrane were visualized by SYTO 24 and counted using a fluorescent microscope in three different fields.

Microscopic analyses

For live cell imaging, cells grown on 12-mm glass-bottomed culture dishes (Iwaki) were transfected with appropriate DNA, at 48 h post-transfection stained with HaloTag -ligand (Promega), NBD C_5-ceramide (Molecular

Probes), Hoechst33342 (Hoechst) or LysoTracker Blue DND-22 (Molecular Probes) according to manufacturer protocols. To detect surface CXCR4 on live cells, cells were incubated with an anti-CXCR4 mAb (A-145) for 30 min at 4°C. In mAb feeding experiments, cells were cultured in medium containing an FITC-conjugated anti-CXCR4 mAb (A-145) and Hoechst, in the presence or absence of 5 μM of cytochalasin D (Sigma). To detect CXCR4, CD63 or FLAG-tagged proteins, cells grown on APS-coated slide glasses (Matsunami) were fixed in 4% (v/v) paraformaldehyde (PFA) for 60 min at 4°C. After washing with PBS, cells were blocked with PBS containing 10% normal donkey serum, followed by an overnight incubation with primary Abs at 4°C. After extensive washing with PBS, cells were incubated with the secondary Abs for 60 min. In case of dual staining, we routinely incubate cells with no, or only one primary Ab, which were served as control for non-specific binding of secondary Abs. To detect CD63, intracellular CXCR4 with intracellular organelle markers or FLAG-tagged CD63ΔN, cells were treated with PBS containing 0.05% saponin for 10 min at room temperature after fixation to enhance permeability. Cells were analyzed at 37°C (live cells) or room temperature (fixed cells) using a 63 / 1.4-0.60 HCX PL APO objective on a DMIRE2-TCS SP2 AOBS confocal microscope system (both from Leica) or a PLAPON 60 O TIRFM objective on a IX71 TIRF microscope system (all from Olympus). Images were acquired and analyzed using LCS 2.61 (Leica) or Basic Metamorph (Molecular Devices) and processed using Photoshop CS2 (Adobe).

Statistical analysis

The Mann–Whitney's *U*-test and Student's *t*-test were used to determine statistical significance, and $P < 0.05$ was considered significant.

Acknowledgments

We thank the many colleagues who have contributed ideas and help to this project, in particular Naoko Misawa, Kuniko Hieda and Shunsuke Hatta for technical support, Chuanyi Nie for discussion, Prof. Kouji Matsushima for providing CXCR4 plasmid DNA, Prof. Hiroshi Sato for providing Myc-MT1-MMP plasmid DNA and Prof. Hiroshi Kimura for teaching us to manipulate TIRFM. The authors declare no competing financial interests. This work was supported by grants from the Ministry of Health, Labor, and Welfare and the Ministry of Education, Culture, Sports, Science and Technology of JAPAN. T. Y. is a research fellow of the Japan Society for the Promotion of Science.

Supplementary Materials

Figure S1: Nucleotide sequence of *cd63* cDNA. Nucleotide sequences of the wild-type *cd63* cDNA, and that of the cDNA clones (12.03 and 12.22) isolated at the outset of this study and newly cloned cDNA for preparing lentiviral vector, are indicated. Capital letters indicate the translated region (the CD63wt ORF starts at 95 and the CD63ΔN ORF starts at 341). Dashed lines indicate positions showing identical nucleotide sequence to the human *cd63* cDNA in the NCBI database (accession number of human *cd63* cDNA, NM_001780).

Figure S2: Subcellular distribution of CXCR4 in empty vector-transduced cells. Co-localization of CXCR4 with intracellular organelles (calnexin; ER, GM130; *cis*-Golgi, LAMP-1; late endosome) was shown in empty vector-transduced MAGIC-5 cells. Images were acquired through band-pass filters (BPF) 500–520 nm (CXCR4: green) and BPF 650–700 nm (intracellular organelles: magenta). Scale bars, 10 μm. Merged images are shown in bottom.

Supplementary experimental procedures: Microscopic analyses.

Supplemental materials are available as part of the online article at http://www.blackwell-synergy.com

References

1. Goff SP. Retrovirus restriction factors. Mol Cell 2004;16:849–859.
2. Kawano Y, Yoshida T, Hieda K, Aoki J, Miyoshi H, Koyanagi Y. A lentiviral cDNA library employing lambda recombination used to clone an inhibitor of human immunodeficiency virus type 1-induced cell death. J Virol 2004;78:11352–11359.
3. Feng Y, Broder CC, Kennedy PE, Berger EA. HIV-1 entry cofactor: functional cDNA cloning of a seven-transmembrane, G protein-coupled receptor. Science 1996;272:872–877.
4. Oberlin E, Amara A, Bachelerie F, Bessia C, Virelizier JL, Arenzana-Seisdedos F, Schwartz O, Heard JM, Clark-Lewis I, Legler DF, Loetscher M, Baggiolini M, Moser B. The CXC chemokine SDF-1 is the ligand for LESTR/fusin and prevents infection by T-cell-line-adapted HIV-1. Nature 1996;382:833–835.
5. Signoret N, Oldridge J, Pelchen-Matthews A, Klasse PJ, Tran T, Brass LF, Rosenkilde MM, Schwartz TW, Holmes W, Dallas W, Luther MA, Wells TN, Hoxie JA, Marsh M. Phorbol esters and SDF-1 induce rapid endocytosis and down modulation of the chemokine receptor CXCR4. J Cell Biol 1997;139:651–664.
6. Cheng ZJ, Zhao J, Sun Y, Hu W, Wu YL, Cen B, Wu GX, Pei G. Beta-arrestin differentially regulates the chemokine receptor CXCR4-mediated signaling and receptor internalization, and this implicates multiple interaction sites between beta-arrestin and CXCR4. J Biol Chem 2000;275:2479–2485.
7. Orsini MJ, Parent JL, Mundell SJ, Benovic JL, Marchese A. Trafficking of the HIV coreceptor CXCR4. Role of arrestins and identification of residues in the c-terminal tail that mediate receptor internalization. J Biol Chem 1999;274:31076–31086.
8. Marchese A, Benovic JL. Agonist-promoted ubiquitination of the G protein-coupled receptor CXCR4 mediates lysosomal sorting. J Biol Chem 2001;276:45509–45512.
9. Marchese A, Raiborg C, Santini F, Keen JH, Stenmark H, Benovic JL. The E3 ubiquitin ligase AIP4 mediates ubiquitination and sorting of the G protein-coupled receptor CXCR4. Dev Cell 2003;5:709–722.
10. Neel NF, Schutyser E, Sai J, Fan GH, Richmond A. Chemokine receptor internalization and intracellular trafficking. Cytokine Growth Factor Rev 2005;16:637–658.
11. Tarrant JM, Robb L, van Spriel AB, Wright MD. Tetraspanins: molecular organisers of the leukocyte surface. Trends Immunol 2003;24:610–617.
12. Escola JM, Kleijmeer MJ, Stoorvogel W, Griffith JM, Yoshie O, Geuze HJ. Selective enrichment of tetraspan proteins on the internal vesicles of multivesicular endosomes and on exosomes secreted by human B-lymphocytes. J Biol Chem 1998;273:20121–20127.
13. Kobayashi T, Vischer UM, Rosnoblet C, Lebrand C, Lindsay M, Parton RG, Kruithof EK, Gruenberg J. The tetraspanin CD63/lamp3 cycles between endocytic and secretory compartments in human endothelial cells. Mol Biol Cell 2000;11:1829–1843.
14. Metzelaar MJ, Wijngaard PL, Peters PJ, Sixma JJ, Nieuwenhuis HK, Clevers HC. CD63 antigen. A novel lysosomal membrane glycoprotein, cloned by a screening procedure for intracellular antigens in eukaryotic cells. J Biol Chem 1991;266:3239–3245.
15. Rous BA, Reaves BJ, Ihrke G, Briggs JA, Gray SR, Stephens DJ, Banting G, Luzio JP. Role of adaptor complex AP-3 in targeting wild-type and mutated CD63 to lysosomes. Mol Biol Cell 2002;13:1071–1082.
16. Berditchevski F, Tolias KF, Wong K, Carpenter CL, Hemler ME. A novel link between integrins, transmembrane-4 superfamily proteins (CD63 and CD81), and phosphatidylinositol 4-kinase. J Biol Chem 1997;272:2595–2598.
17. Jung KK, Liu XW, Chirco R, Fridman R, Kim HR. Identification of CD63 as a tissue inhibitor of metalloproteinase-1 interacting cell surface protein. EMBO J 2006;25:3934–3942.

18. Latysheva N, Muratov G, Rajesh S, Padgett M, Hotchin NA, Overduin M, Berditchevski F. Syntenin-1 is a new component of tetraspanin-enriched microdomains: mechanisms and consequences of the interaction of syntenin-1 with CD63. Mol Cell Biol 2006;26:7707–7718.
19. Duffield A, Kamsteeg EJ, Brown AN, Pagel P, Caplan MJ. The tetraspanin CD63 enhances the internalization of the H,K-ATPase beta-subunit. Proc Natl Acad Sci U S A 2003;100:15560–15565.
20. Takino T, Miyamori H, Kawaguchi N, Uekita T, Seiki M, Sato H. Tetraspanin CD63 promotes targeting and lysosomal proteolysis of membrane-type 1 matrix metalloproteinase. Biochem Biophys Res Commun 2003;304:160–166.
21. Levy S, Shoham T. The tetraspanin web modulates immune-signalling complexes. Nat Rev Immunol 2005;5:136–148.
22. Hemler ME. Tetraspanin functions and associated microdomains. Nat Rev Mol Cell Biol 2005;6:801–811.
23. Stipp CS, Kolesnikova TV, Hemler ME. Functional domains in tetraspanin proteins. Trends Biochem Sci 2003;28:106–112.
24. Miura Y, Misawa N, Kawano Y, Okada H, Inagaki Y, Yamamoto N, Ito M, Yagita H, Okumura K, Mizusawa H, Koyanagi Y. Tumor necrosis factor-related apoptosis-inducing ligand induces neuronal death in a murine model of HIV central nervous system infection. Proc Natl Acad Sci U S A 2003;100:2777–2782.
25. Endres MJ, Clapham PR, Marsh M, Ahuja M, Turner JD, McKnight A, Thomas JF, Stoebenau-Haggarty B, Choe S, Vance PJ, Wells TN, Power CA, Sutterwala SS, Doms RW, Landau NR et al. CD4-independent infection by HIV-2 is mediated by fusin/CXCR4. Cell 1996;87:745–756.
26. Futahashi Y, Komano J, Urano E, Aoki T, Hamatake M, Miyauchi K, Yoshida T, Koyanagi Y, Matsuda Z, Yamamoto N. Separate elements are required for ligand-dependent and -independent internalization of metastatic potentiator CXCR4. Cancer Sci 2007;98:373–379.
27. von Lindern JJ, Rojo D, Grovit-Ferbas K, Yeramian C, Deng C, Herbein G, Ferguson MR, Pappas TC, Decker JM, Singh A, Collman RG, O'Brien WA. Potential role for CD63 in CCR5-mediated human immunodeficiency virus type 1 infection of macrophages. J Virol 2003;77:3624–3633.
28. Ho SH, Martin F, Higginbottom A, Partridge LJ, Parthasarathy V, Moseley GW, Lopez P, Cheng-Mayer C, Monk PN. Recombinant extracellular domains of tetraspanin proteins are potent inhibitors of the infection of macrophages by human immunodeficiency virus type 1. J Virol 2006;80:6487–6496.
29. Jourdan P, Abbal C, Noraz N, Hori T, Uchiyama T, Vendrell JP, Bousquet J, Taylor N, Pene J, Yssel H. IL-4 induces functional cell-surface expression of CXCR4 on human T cells. J Immunol 1998;160:4153–4157.
30. Hewitt EW. The MHC class I antigen presentation pathway: strategies for viral immune evasion. Immunology 2003;110:163–169.
31. Schwartz O, Marechal V, Le Gall S, Lemonnier F, Heard JM. Endocytosis of major histocompatibility complex class I molecules is induced by the HIV-1 Nef protein. Nat Med 1996;2:338–342.
32. Piguet V, Wan L, Borel C, Mangasarian A, Demaurex N, Thomas G, Trono D. HIV-1 Nef protein binds to the cellular protein PACS-1 to downregulate class I major histocompatibility complexes. Nat Cell Biol 2000;2:163–167.
33. Andersson M, Paabo S, Nilsson T, Peterson PA. Impaired intracellular transport of class I MHC antigens as a possible means for adenoviruses to evade immune surveillance. Cell 1985;43:215–222.
34. Hudson AW, Howley PM, Ploegh HL. A human herpesvirus 7 glycoprotein, U21, diverts major histocompatibility complex class I molecules to lysosomes. J Virol 2001;75:12347–12358.
35. Reusch U, Muranyi W, Lucin P, Burgert HG, Hengel H, Koszinowski UH. A cytomegalovirus glycoprotein re-routes MHC class I complexes to lysosomes for degradation. EMBO J 1999;18:1081–1091.
36. Berditchevski F, Odintsova E. Tetraspanins as regulators of protein trafficking. Traffic 2007;8:89–96.
37. Signoret N, Rosenkilde MM, Klasse PJ, Schwartz TW, Malim MH, Hoxie JA, Marsh M. Differential regulation of CXCR4 and CCR5 endocytosis. J Cell Sci 1998;111:2819–2830.
38. Shoham T, Rajapaksa R, Kuo CC, Haimovich J, Levy S. Building of the tetraspanin web: distinct structural domains of CD81 function in different cellular compartments. Mol Cell Biol 2006;26:1373–1385.
39. Maecker HT, Levy S. Normal lymphocyte development but delayed humoral immune response in CD81-null mice. J Exp Med 1997;185:1505–1510.
40. Miyazaki T, Muller U, Campbell KS. Normal development but differentially altered proliferative responses of lymphocytes in mice lacking CD81. EMBO J 1997;16:4217–4225.
41. Hachiya A, Aizawa-Matsuoka S, Tanaka M, Takahashi Y, Ida S, Gatanaga H, Hirabayashi Y, Kojima A, Tatsumi M, Oka S. Rapid and simple phenotypic assay for drug susceptibility of human immunodeficiency virus type 1 using CCR5-expressing HeLa/CD4( ) cell clone 1-10 (MAGIC-5). Antimicrob Agents Chemother 2001;45:495–501.
42. Tanaka R, Yoshida A, Murakami T, Baba E, Lichtenfeld J, Omori T, Kimura T, Tsurutani N, Fujii N, Wang ZX, Peiper SC, Yamamoto N, Tanaka Y. Unique monoclonal antibody recognizing the third extracellular loop of CXCR4 induces lymphocyte agglutination and enhances human immunodeficiency virus type 1-mediated syncytium formation and productive infection. J Virol 2001;75:11534–11543.
43. Dougherty JP, Wisniewski R, Yang SL, Rhode BW, Temin HM. New retrovirus helper cells with almost no nucleotide sequence homology to retrovirus vectors. J Virol 1989;63:3209–3212.
44. Kawano Y, Tanaka Y, Misawa N, Tanaka R, Kira JI, Kimura T, Fukushi M, Sano K, Goto T, Nakai M, Kobayashi T, Yamamoto N, Koyanagi Y. Mutational analysis of human immunodeficiency virus type 1 (HIV-1) accessory genes: requirement of a site in the nef gene for HIV-1 replication in activated CD4 T cells in vitro and in vivo. J Virol 1997;71:8456–8466.
45. Zack JA, Arrigo SJ, Weitsman SR, Go AS, Haislip A, Chen IS. HIV-1 entry into quiescent primary lymphocytes: molecular analysis reveals a labile, latent viral structure. Cell 1990;61:213–222.

JOURNAL OF VIROLOGY, Jan. 2008, p. 1021–1033 Vol. 82, No. 2
0022-538X/08/$08.00 0 doi:10.1128/JVI.01044-07

Modulation of Human Immunodeficiency Virus Type 1 Infectivity through Incorporation of Tetraspanin Proteins

Kei Sato,[1] Jun Aoki,[1,2] Naoko Misawa,[1] Eriko Daikoku,[3] Kouichi Sano,[3] Yuetsu Tanaka,[4] and Yoshio Koyanagi[1]*

Laboratory of Viral Pathogenesis, Institute for Virus Research, Kyoto University, Sakyo-ku, Kyoto, Kyoto 606-8507, Japan[1]; Department of Immunology, Tohoku University Graduate School of Medicine, Aoba-ku, Sendai, Miyagi 980-8575, Japan[2]; Department of Preventive and Social Medicine, Osaka Medical College, Takatsuki, Osaka 569-8686, Japan[3]; and Department of Immunology, Graduate School of Medicine, University of the Ryukyus, Nishihara, Okinawa 903-0215, Japan[4]

Received 14 May 2007/Accepted 27 October 2007

Accumulating evidence indicates that human immunodeficiency virus type 1 (HIV-1) acquires various cellular membrane proteins in the lipid bilayer of the viral envelope membrane. Although some virion-incorporated cellular membrane proteins are known to potently affect HIV-1 infectivity, the virological functions of most virion-incorporated membrane proteins remain unclear. Among these host proteins, we found that CD63 was eliminated from the plasma membranes of HIV-1-producing T cells after activation, followed by a decrease in the amount of virion-incorporated CD63, and in contrast, an increase in the infectivity of the released virions. On the other hand, we found that CD63 at the cell surface was preferentially embedded on the membrane of released virions in an HIV-1 envelope protein (Env)-independent manner and that virion-incorporated CD63 had the potential to inhibit HIV-1 Env-mediated infection in a strain-specific manner at the postattachment entry step(s). In addition, these behaviors were commonly observed in other tetraspanin proteins, such as CD9, CD81, CD82, and CD231. However, L6 protein, whose topology is similar to that of tetraspanins but which does not belong to the tetraspanin superfamily, did not have the potential to prevent HIV-1 infection, despite its successful incorporation into the released particles. Taken together, these results suggest that tetraspanin proteins have the unique potential to modulate HIV-1 infectivity through incorporation into released HIV-1 particles, and our findings may provide a clue to undiscovered aspects of HIV-1 entry.

To initiate the infection of human immunodeficiency virus type 1 (HIV-1), the envelope protein (Env) plays a critical role in mediating the attachment of virions to target cells and the following fusion with the cellular membrane (24). HIV-1 Env is composed of the surface protein (gp120) and the transmembrane protein (gp41). gp120 binds first to its primary receptor, CD4 (15, 37), and subsequently to its coreceptor, CXCR4 or CCR5 (10, 17, 19, 20, 22). Thereafter, the ectodomain of gp41 executes fusion of viral envelope and the plasma membrane of target cell (24). Therefore, the incorporation of Env into released virion is a key step in acquiring infectivity.

During the budding process of HIV-1, not only HIV-1 Env but also a variety of cellular membrane proteins are efficiently incorporated into released progeny virions (7), and some of them are involved in HIV-1 infection. For example, HIV-1 infectivity is enhanced by virion-incorporated proteins, such as human leukocyte antigens (HLAs) (6, 13, 44), costimulatory molecules (CD80 and CD86) (21, 25), and intracellular adhesion molecule-1 (ICAM-1) (2, 4). Since their individual counterreceptors are expressed on the surface of HIV-1 target cells, it is thought that the interaction between these membrane proteins on virions and their counterreceptors on target cells facilitates the association of viral particles and the target cells. In addition, virion-incorporated ICAM-1 also has the potential to contribute to virus-to-cell fusion (67). In contrast, it has been shown that CD4 proteins have the potential to prevent HIV-1 infection at the attachment step through incorporation into the released particles (66). Furthermore, there is a report indicating that HIV-1 particles are protected by glycosylphosphatidylinositol-anchored complement control proteins, such as CD55 and CD59, which have the physiological function of preventing the assembly of the membrane attack complex (61). They are inserted into HIV-1 virions and then protect them from complement-mediated viral lysis. However, the virological and immunological functions of most of the other virion-incorporated membrane proteins remain unclear.

CD63 is one of the cellular membrane proteins that are incorporated into HIV-1 virions (9, 46, 55). CD63 is a type II cellular membrane protein and belongs to the tetraspanin superfamily (32, 62). It has been reported that CD63 colocalizes with Gag protein in HIV-1-producing cells (3, 28, 52, 55, 56, 60). In addition, Nydegger et al. showed that CD63 forms tetraspanin-enriched microdomains (TEMs) that collaborate with other tetraspanin proteins, such as CD9, CD81, and CD82, and that TEMs act as the gateway for HIV-1 budding at the plasma membrane (50). Furthermore, Jolly and Sattentau reported that TEM components are accumulated on the sur-

* Corresponding author. Mailing address: Laboratory of Viral Pathogenesis, Institute for Virus Research, Kyoto University, 53 Shogoinkawara-cho, Sakyo-ku, Kyoto, Kyoto 606-8507, Japan. Phone: 81-75-751-4811. Fax: 81-75-751-4812. E-mail: ykoyanag@virus.kyoto-u.ac.jp.

Published ahead of print on 7 November 2007.

faces of HIV-1-producing CD4 T cells and colocalize with HIV-1 Env and Gag (35).

Recently, it was suggested that CD63 plays roles in HIV-1 replication. For example, Lindern et al. reported that the pretreatment of macrophages with anti-CD63 antibodies inhibits HIV-1 infection (70). In addition, Ho et al. have shown that the recombinant soluble protein of the large extracellular loop (LEL) of CD63 potently inhibits HIV-1 infection to macrophages, presumably at the entry step (33). Nevertheless, the practical role(s) and function(s) of intact CD63 protein in HIV-1 infection are still unclear.

Here, we investigated whether CD63 has any virological function in HIV-1 infection. We observed that CD63 was removed from the plasma membrane of HIV-1-producing T cells by activation stimuli, and that the activated cells released HIV-1 virions that contained smaller amounts of CD63 and had higher infectivity. In addition, through exogenous expression experiments, we found evidence suggesting that CD63 at the plasma membrane of HIV-1-producing cells was efficiently incorporated into released virions and that virion-incorporated CD63 had the potential to impair HIV-1 Env-mediated infection in a strain-specific manner at the postattachment step(s). Similar behavior was also observed in other tetraspanin proteins, such as CD9, CD81, CD82, and CD231. However, L6, which has topology similar to that of tetraspanins but does not belong to the tetraspanin superfamily, did not have the potential to prevent HIV-1 infection. These are the first findings suggesting that some cellular membrane proteins can attenuate HIV-1 Env-mediated infection in a strain-specific manner through incorporation into released HIV-1 particles.

MATERIALS AND METHODS

Cells. 293T cells and MAGIC-5 cells (HeLa cells transduced with genes for CD4, CCR5, and long terminal repeat-driving -galactosidase) (29) were maintained in Dulbecco's modified Eagle medium containing 10% fetal calf serum (FCS), 100 U/ml penicillin, and 100 g/ml streptomycin. Molt4/IIIB cells, which persistently produce HIV-1_{IIIB} (39), and MT-4 cells were maintained in RPMI 1640 medium containing 10% FCS, 100 U/ml penicillin, and 100 g/ml streptomycin. To activate Molt4/IIIB cells, 1 g/ml phytohemagglutinin (PHA) and 100 ng/ml phorbol 12-myristate 13-acetate (PMA) were added, and cells were cultured for 72 h. To prepare activated primary CD4 T cells, peripheral blood mononuclear cells (PBMCs) were isolated from peripheral blood of healthy HIV-1-seronegative donors as previously described (41). CD4 T cells were isolated from the PBMCs by using a CD4-positive-cell isolation kit (Dynal, Oslo, Norway) and were activated by using a Dynabeads CD3/CD28 T-cell expander (Dynal) according to the manufacturer's instructions. Activated primary CD4 T cells were maintained in RPMI 1640 containing 10% FCS, 100 U/ml interleukin-2 (Shionogi, Osaka, Japan), 100 U/ml penicillin, and 100 g/ml streptomycin.

Plasmid construction. To construct a CD63 expression plasmid (pCD63), a *cd63* cDNA fragment was amplified by PCR from a human leukocyte cDNA library (Invitrogen, Carlsbad, CA) using the following primers: sense, 5 -TA GCG AAT TCC ATG GCG GTG GAA GGA G-3 ; antisense, 5 -TA GCT CTA GAC CTA CAT CAC CTC GTA GCC ACT-3 . The resulting fragment was digested with EcoRI and XbaI and inserted into the EcoRI-XbaI site of pCMV-SPORT6 (Invitrogen). To construct CD9-, CD81-, CD82-, and CD231-expressing plasmids (pCD9, pCD81, pCD82, and pCD231), *cd9*, *cd81*, *cd82*, and *cd231* cDNA fragments were obtained similarly, using the following primers: *cd9* sense, 5 -TT TTG AAT TCC ATG CCG GTC AAA GGA GGC A-3 ; *cd9* antisense, 5 -TT TTT GAT ATC CTA GAC CAT CTC GCG GTT CCT-3 ; *cd81* sense, 5 -TT TTG AAT TCC ATG GGA GTG GAG GGC TGC A-3 ; *cd81* antisense, 5 -TT TTT GAT ATC TCA GTA CAC GGA GCT GTT CCG GAT-3 ; *cd82* sense, 5 -TT TTG AAT TCC ATG GGC TCA GCC TGT ATC AAA G-3 ; *cd82* antisense, 5 -TT TTT GAT ATC TCA GTA CTT GGG GAC CTT GCT GT A-3 ; *cd231* sense, 5 -TT TTG GTA CCC ATG GCA TCG AGG AGA ATG GA-3 ; *cd231* antisense, 5 -TT TTT GAT ATC TTA CAC CAT CTC ATA CTG ATT GGC-3 . The *cd9* cDNA fragment was also amplified from the leukocyte library, whereas *cd81*, *cd82*, and *cd231* cDNA fragments were obtained by reverse transcription-PCR of mRNA derived from Jurkat cells. These cDNA fragments were digested with EcoRI and EcoRV and inserted into the EcoRI-EcoRV site of pCMV-SPORT6. To construct an L6-expressing plasmid (pL6), *l6* cDNA was obtained from pRcCMV-L6 (kindly provided by E. Mekada) using the following primers: *l6* sense, 5 -TT TTG GTA CCC ATG TGC TAT GGG AAG TGT GCA-3 ; *l6* antisense, 5 -TT TTT GAT ATC TTA GCA GTC ATA TTG CTG TTG GTG-3 . The resulting fragment was digested with KpnI and EcoRI and inserted into the KpnI-EcoRI site of pCMV-SPORT6. To construct pCD63 L, expressing a CD63 with the lysosomal sorting motif deleted (CD63 L), pCD63 was digested with PstI and XbaI, and the following mutagenic oligonucleotides were inserted: sense, 5 -GCA GCC CTT GGA ATT GCT TTT GTC GAG GTT TTG GGA ATT GTC TTT GCC TGC TGC CTC GTG AAG AGT ATC AGA TAG T-3 ; antisense, 5 -CT AGA CTA TCT GAT ACT CTT CAC GAG GCA GCA GGC AAA GAC AAT TCC CAA AAC CTC GAC AAA AGC AAT TCC AAG GGC TGC TGC A-3 . To construct pJRFLenv, a HindIII-XhoI fragment containing HIV-1_{JR-FL} *tat*, *rev*, and *env* was inserted into pGEM4 (Promega, Madison, WI). To construct pNL4-3 env (which lacks HIV-1_{NL4-3} *env*), pNL4-3 was digested with NheI, blunted, and self-ligated. PCR was carried out with the Expand Long Template PCR system (Roche, Mannheim, Germany), and reverse transcription-PCR was carried out by using SuperScript One-Step RT-PCR with Platinum high-fidelity *Taq* (Invitrogen), according to the manufacturer's protocols. Sequences of these plasmid constructs were confirmed with an ABI Prism 3100 genetic analyzer (Applied Biosystems, Foster City, CA).

Virus preparation. 293T cells were seeded to appropriate densities 1 day prior to transfection and were transfected by the calcium phosphate method as described previously (36). The culture supernatants were harvested, centrifuged, and then filtrated to produce virus solutions at 48 h posttransfection. To prepare HIV-1 and virus-like particles (VLPs), cells were cotransfected with pNL4-3 (1), pJR-FL (40), pNLFLV3 (kindly provided by W. A. O'Brien) (63), pNL4-3 env, and either tetraspanin-expressing plasmids or pCMV-SPORT6 (empty vector). To prepare pseudotyped viruses with envelope protein (Env) from either HIV-1 (NL4-3, IIIB, JR-FL, and NL4-3 CT, which encodes an NL4-3 Env with a deletion of the cytoplasmic tail [CT]) or vesicular stomatitis virus (VSV), cells were cotransfected with the Env expression plasmid DNA, pIIINL4env (kindly donated by T. Murakami and E. O. Freed) (48), pLET (59), pJRFLenv, pIIINL4envCTdel-144-2 (kindly donated by T. Murakami and E. O. Freed) (48), or pMD.G (53), respectively, and with pNLLuc (an Env-defective HIV-1_{NL4-3} carrying the luciferase gene) (57) and either tetraspanin-expressing plasmids or empty vector. To prepare -lactamase (BlaM)-conjugated Vpr-containing NL4-3 (NL4-$3^{BlaM-Vpr}$), pNL4-3 and pCMV4-3BlaM-Vpr (kindly provided by W. C. Greene) (8) were cotransfected with pCD63 or empty vector. To prepare HIV-1_{IIIB}, culture supernatants of Molt4/IIIB cells were harvested, centrifuged, and then filtered to produce virus solutions.

Antibodies and reagents. The following antibodies and reagents were used in this study: anti-CD63 mouse monoclonal antibody (mMAb) (MX-49.129.5; Santa Cruz Biotechnology, Santa Cruz, CA); anti-CD9 mMAb (M-L13; BD Biosciences, San Jose, CA); anti-CD81 mMAb (1D6; Serotec, Oxford, United Kingdom); anti-CD82 mMAb (B-L2; Serotec); anti-CD231 mMAb (H1-A12; BD Biosciences); anti-L6 mMAb (D1-D2; Chemicon, Temecula, CA); anti-CD45 mMAb (H130; BD Biosciences); anti- -actin mMAb (AC-15; Sigma, St. Louis, MO); rat anti-gp120 MAb (W#10, which recognizes the V3 region of HIV_{IIIB} Env [Y. Tanaka, unpublished data]); goat anti-$p24^{CA}$ antiserum (ViroStat, Portland, ME); anti-$p17^{MA}$ mMAb (Applied Biotechnologies, Columbia, MD), which recognizes $p17^{MA}$ but not $Pr55^{Gag}$ (51); anti-Vpr mMAb (8D1; kindly donated by Y. Ishizaka); biotinylated horse anti-mouse immunoglobulin G (IgG) Ab (Vector Laboratories, Burlingame, CA); biotinylated donkey anti-rat IgG Ab (Rockland, Gilbertsville, PA); biotinylated donkey anti-goat IgG Ab (Chemicon); biotinylated donkey anti-rabbit IgG Ab (Chemicon); horseradish peroxidase-conjugated horse anti-mouse IgG Ab (Cell Signaling, Denver, MA); horseradish peroxidase-conjugated streptavidin (SA; Zymed, San Francisco, CA); and Alexa Fluor 488-conjugated goat anti-mouse IgG Ab (Molecular Probes, Eugene, OR).

Flow cytometry. In brief, cells were suspended in phosphate-buffered saline (PBS) and incubated for 30 min with appropriate antibodies at 4°C. Flow cytometry was performed with a FACScan (BD Biosciences), and data were analyzed using CellQuest software (BD Biosciences).

Immunoelectron microscopy. Cells were fixed with 0.2% glutaraldehyde in 150 mM PBS (pH 7.2) for 3 min at room temperature and harvested. The collected cells were fixed again with 1% glutaraldehyde in 150 mM PBS at 4°C for 60 min, dehydrated in a graded ethanol series, and embedded in Lowicryl K4M resin. Ultrathin sections were prepared using an ultramicrotome Reichert-Nissei Ul-

tracut-N (Leica, Vienna, Austria), and mounted on a nickel grid supported by a carbon-coated collodion film. The sections on the grid were treated with 5% goat serum in 150 mM PBS (pH 7.2) to block nonspecific reactions. The sections were treated with anti-CD63 mMAb at room temperature for 180 min. After washing three times, the sections were treated with goat serum containing 5-nm colloidal gold-labeled anti-mouse IgG (Amersham, Little Chalfont, United Kingdom) at room temperature for 60 min and washed in PBS. The immunostained sections were fixed with 1% glutaraldehyde in 50 mM cacodylate buffer again and washed in distilled water. The immunolabeled sections were treated with a mixture of 0.01% ruthenium red and 0.5% osmium tetroxide in 50 mM cacodylate buffer at room temperature for 10 min and double stained with uranyl acetate for 20 min, as previously described (38). The sections were observed under an electron microscope (H-7650; Hitachi, Ibaraki, Japan).

Western blotting and slot blotting. Cells were lysed with lysis buffer (1% Triton X-100, 50 mM Tris-HCl [pH 8.0], 150 mM NaCl, and protease inhibitor complete cocktail [Roche]). Virions were concentrated by ultracentrifugation at 100,000 *g* for 1 h at 4°C, and pellets were lysed with lysis buffer. For Western blotting, lysates were separated by sodium dodecyl sulfate-polyacrylamide gel electrophoresis and transferred to Immobilon transfer membranes (Millipore, Bedford, MA). For detection, appropriate antibodies were used. Slot blotting was performed with a Hybri-slot Manifold (Invitrogen), according to the manufacturer's instructions.

Virus titration. IIIB was titrated by 50% tissue culture infective dose ($TCID_{50}$), and the infectious units (IU) of NL4-3, JR-FL, and NLFLV3 were measured by Magi assay, as follows.

(i) $TCID_{50}$. Virus solutions (HIV-1_{IIIB}) were serially diluted with RPMI 1640, and each solution was inoculated onto 6 10^4 MT-4 cells in quadruplicate. The $TCID_{50}$ was calculated as previously described (31).

(ii) Magi assay. MAGIC-5 cells (3 10^4) were seeded into a 24-well plate, 24 h before infection. Virus solutions (HIV-1_{NL4-3}, HIV-1_{JR-FL}, and HIV-1_{NLFLV3}) were diluted appropriately, 200 l of the solutions was inoculated onto MAGIC-5 cells, and cells were incubated for 2 h at 37°C in a CO_2 incubator. After infection, 1 ml of conditioned medium was added for quenching, and the culture was further incubated for 48 h under the same conditions. Cells were fixed in fixing solution (1% formaldehyde, 0.2% glutaraldehyde in PBS) at 48 h postinfection and then treated with staining solution (400 g/ml X-Gal [5-bromo-4-chloro-3-indolyl- -D-galactopyranoside], 4 mM potassium ferrocyanide, 4 mM potassium ferricyanide, 2 mM $MgCl_2$ in PBS). Blue-stained cells in each well were counted in five fields, and the IU were calculated as previously described (29).

ELISA. To quantify $p24^{CA}$ in virus solutions, an HIV-1 p24 antigen enzyme-linked immunosorbent assay (ELISA) kit (ZetroMetrix, Buffalo, NY) was used according to the manufacturer's instructions.

Virus precipitation assay. Virus immunoprecipitation was performed as described previously (21), with some modifications. In brief, virus solution (100 ng of $p24^{CA}$) in PBS containing 3% bovine serum albumin (BSA) was incubated with 1 g of each Ab overnight at 4°C. To harvest the virus-Ab complex, 25 l of Dynabeads protein G (Dynal) in 3% BSA in PBS was added, and the mixture was held for 30 min at room temperature. The captured viruses were then precipitated with a magnet, washed with 3% BSA in PBS, and lysed with lysis buffer. $p24^{CA}$ was quantified by ELISA, as described above, and the amount of bound virions was calculated.

Pseudotyped virus infection and luciferase assay. To measure the infectivity of NL4-3 Env, IIIB Env, and NL4-3 CT Env-pseudotyped virus, MAGIC-5 cells (2 10^5) or MT-4 cells (1.5 10^5) were incubated for 48 h in an aliquot of each virus solution, containing 5 ng or 0.5 ng of $p24^{CA}$. A solution of JR-FL Env-pseudotyped virus, containing 20 ng of $p24^{CA}$, was incubated with MAGIC-5 cells (1 10^5) for 72 h. A solution of VSV envelope glycoprotein (VSV-G)-pseudotyped virus, containing 0.5 ng of $p24^{CA}$, was incubated with both MAGIC-5 cells (2 10^5) and MT-4 cells (1.5 10^5) for 48 h. Activated primary CD4 T cells (1 10^6) were inoculated with NL4-3 Env-pseudotyped virus, containing 10 ng of $p24^{CA}$, and incubated for 48 h. The Picagene luciferase assay kit (Toyo Ink, Tokyo, Japan) was used to perform luciferase assays, following the manufacturer's protocols. Activity was measured with a 1420 ARVOSX multilabel counter (Perkin Elmer, Wellesley, MA) and normalized to the protein content of each lysate, measured with a Coomassie (Bradford) protein assay kit (Pierce, Rockford, IL). All experiments were performed in triplicate.

Virus attachment assay. The virus attachment assay was performed as described previously (66) with some modifications. In brief, MT-4 cells (2 10^5) were incubated for 2 h at 4°C with an aliquot of HIV-1 containing 10 ng of $p24^{CA}$. After the incubation, cells were washed once with chilled Dulbecco's modified Eagle medium and five times with chilled PBS before being lysed with lysis buffer. The amounts of $p24^{CA}$ in these lysates were determined by ELISA, as described above, and the amount of attached virions was calculated.

HIV-1 fusion assay. The HIV-1 fusion assay, which is based on the incorporation of -lactamase–Vpr chimeric proteins (BlaM-Vpr) into virions and subsequent BlaM cleavage of a fluorescent dye (CCF2) present in target cells, was performed as described previously (8). In brief, MT-4 cells (5 10^5) were incubated for 3 h at 37°C in a CO_2 incubator, with aliquots of NL4-$3^{BlaM-Vpr}$ containing 100 ng of $p24^{CA}$. Cells were washed once with an equilibrated buffer (RPMI 1640 containing 10% FCS and 20 mM HEPES-NaOH [pH 7.4]) and then incubated in 100 l of substrate loading buffer (2 M CCF2-AM in the equilibrated buffer, prepared according to the manufacturer's instructions [Invitrogen]) for 1 h at room temperature. After washing twice with the equilibrated buffer, cells were incubated in an equilibrated buffer containing 2.5 mM probenecid (Sigma) for 7 h at room temperature, to allow the BlaM reaction to develop. Finally, cells were washed once with PBS and fixed in 1% formalin neutral buffer solution. The change in emission fluorescence of the CCF2 dye, following its cleavage by BlaM-Vpr, was monitored by flow cytometry with FACSAria (BD Biosciences). Data were analyzed with FACSDiva software (BD Biosciences) and evaluated as previously described (8).

Real-time PCR. The amount of HIV-1 reverse transcripts (RT) was determined as previously described (64). In brief, to completely remove contaminating transfected pNL4-3 plasmid DNA, the virus solution was preincubated with DNase I (3,500 U/ml; Takara Bio, Shiga, Japan) containing 10 mM $MgCl_2$ for 30 min at room temperature. MT-4 cells (4 10^5) were incubated for 2 h at 37°C with aliquots of HIV-1 containing 2 ng of $p24^{CA}$. After infection, the cells were vigorously washed and cultured for 3 or 6 h. DNA was extracted by the urea-lysis method, and 500 ng of DNA was used as the template. Real-time PCR was performed by using a 7500 real-time system (Applied Biosystems), and data were analyzed with 7500 system SDS software (Applied Biosystems) and evaluated as previously described (64).

Statistical analysis. Student's *t* test was used to determine statistical significance. *P* values of 0.05, 0.01, and 0.001 were considered significant.

RESULTS

Activation of Molt4/IIIB cells intensifies HIV-1 infectivity and eliminates CD63 from both the released virions and the plasma membrane. The activation stimulus causes augmentation of HIV-1 production (30, 74). We stimulated Molt4/IIIB cells, which persistently produce infectious HIV-1_{IIIB} virions (39), with PHA and PMA and detected a threefold increase in the amount of $p24^{CA}$ released into the culture supernatant, as measured by ELISA (Fig. 1A). Interestingly, we also found that PHA/PMA activation significantly enhanced the infectivity of released HIV-1_{IIIB} virions (Fig. 1B). We first suspected that it might have been caused by the increase in the amount of mature HIV-1 Env, gp120, incorporated into HIV-1 particles. However, as shown in Fig. 1C, there was little change in the amount of gp120. Instead, the virus precipitation assay (21) revealed a large reduction in the virion-incorporated CD63 (Fig. 1D). As one of negative controls for this assay, we used an anti-CD45 antibody. It has already been proven that CD45 is expressed on the plasma membrane of leukocytes but is hardly incorporated into HIV-1 particles (49, 69). As previously reported, this antibody did not capture HIV-1 particles (Fig. 1D), suggesting that our assay specifically captured CD63 protein on the released HIV-1 particles. Correspondingly, we observed that CD63 expression on the surface of Molt4/IIIB cells was significantly down-modulated following PHA/PMA activation (Fig. 1E and F). As we suspected that the decrease of CD63 on virus particles might be related to the enhancement of virus infectivity, in subsequent experiments, we investigated the role of CD63 in the modulation of HIV-1 infectivity.

CD63 is incorporated into virions in an Env-independent manner and reduces infectivity. To directly examine the po-

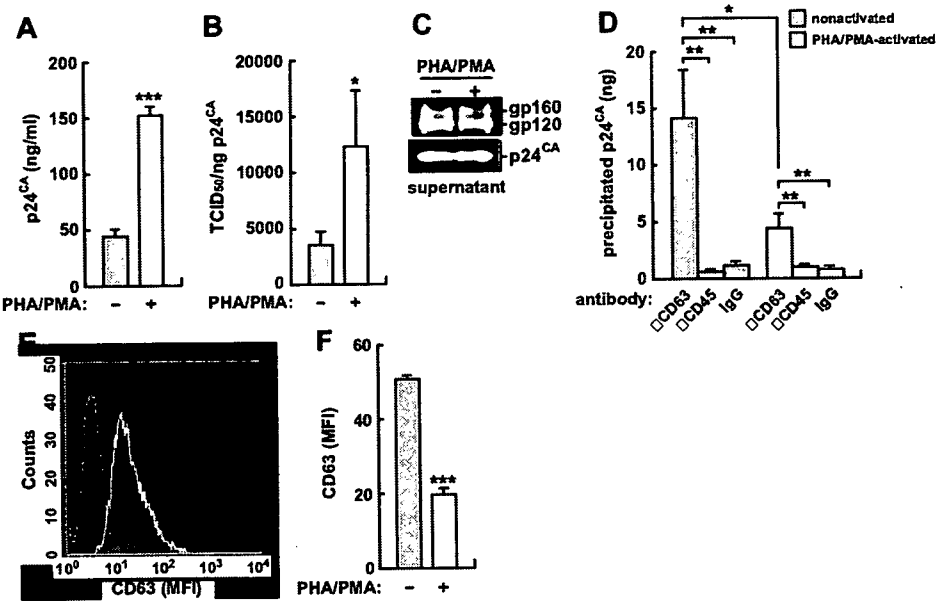

FIG. 1. Inverse correlation between HIV-1 infectivity and the level of CD63 in the released virions. Molt4/IIIB cells were activated with PHA (1 g/ml) and PMA (100 ng/ml) for 72 h. (A) HIV-1_{IIIB} particles released from nonactivated or PHA/PMA-activated Molt4/IIIB cells were quantitated by $p24^{CA}$ ELISA. (B) The $TCID_{50}$ was measured as described in Materials and Methods and was normalized to the amount to $p24^{CA}$. (C) The level of Env in HIV-1_{IIIB} particles was analyzed by Western blotting. The input was standardized to $p24^{CA}$, and a representative result is shown. (D) The virus precipitation assay was performed as described in Materials and Methods. HIV-1_{IIIB} particles (100 ng of $p24^{CA}$) released from nonactivated or PHA/PMA-activated Molt4/IIIB cells were used for immunoprecipitation by respective antibodies. (E and F) The surface expression of CD63 on nonactivated (filled in gray) and PHA/PMA-activated (black line) Molt4/IIIB cells was analyzed by flow cytometry. Isotype IgG was used as a negative control (broken line). A representative result is shown in panel E, and summarized results are shown in panel F. Experiments were performed in triplicate. Statistical significance (Student's *t* test) is shown as follows: *, P 0.05; **, P 0.01; ***, P 0.001. Error bars indicate standard deviations. MFI, mean fluorescence intensity.

tential of virion-incorporated CD63, we cotransfected a CD63 expression plasmid (pCD63) and pNL4-3 into 293T cells. Western blotting analyses showed that exogenous expression of CD63 did not influence the expression of HIV-1 components (Fig. 2A, top) and that there was little change in either the amount of released HIV-1 particles (Fig. 2C) or the detected HIV-1 components, including Env (gp120 and gp160), Gag (precursor protein [$Pr55^{Gag}$], cleavage intermediate [$p41^{MA-CA}$], $p24^{CA}$, and $p17^{MA}$), and Vpr (Fig. 2A, bottom). In addition, pNL4-3 transfection did not affect the surface expression of CD63, and exogenous CD63 was successfully expressed on the surfaces of 293T cells (Fig. 2B). In the virus precipitation assay, we observed that the level of endogenous CD63 on conventional HIV-1_{NL4-3} particles (Fig. 2D) was similar to that on HIV-1_{IIIB} particles released from PHA/PMA-activated Molt4/IIIB cells (Fig. 1D). Likewise, exogenous CD63 was efficiently incorporated into the released HIV-1_{NL4-3} (Fig. 2D) in amounts comparable to those in HIV-1_{IIIB} released from nonactivated Molt4/IIIB cells (Fig. 1D). These observations suggest that this 293T cell system may be an appropriate system for studying the phenomenon in Molt4/IIIB cells. Moreover, immunoelectron microscopy with an anti-CD63 antibody confirmed the presence of endogenous CD63 in HIV-1 particles (Fig. 2F), and the amount of virion-incorporated CD63 was increased by the exogenous expression (Fig. 2G). To analyze the necessity of Env for incorporation CD63 into released virions, we cotransfected cells with pCD63 and pNL4-3 env, which lacks NL4-3 *env* and produces virus-like particles. As shown in Fig. 2E, the level of CD63 on virus-like particles was comparable to that in wild-type NL4-3. Because ICAM-1 and HLA-DR are incorporated into released HIV-1 particles in an Env-independent manner (2, 44), it would not be surprising to find that Env is dispensable for the incorporation of CD63 into the released HIV-1 virions.

To investigate the virions released from pCD63-transfected cells further, we measured infectivity with a Magi assay (29). Although $p24^{CA}$ ELISA indicated that the amounts of released virions were comparable (Fig. 2C), the Magi assay revealed that the virions released from pCD63-transfected cells were significantly less infectious than typical virions (Fig. 2H). These results suggest that CD63 proteins on HIV-1 particles may have a suppressive effect on HIV-1 infection.

Non-virion-associated CD63 has no effect on HIV-1 infection. As shown in Fig. 2A, we observed that CD63 proteins are also released from the cells transfected solely with pCD63. It was recently reported that recombinant large extracellular domains of tetraspanin proteins, including CD63, potently inhibit HIV-1 infection (33). To eliminate the possibility that the infectivity reduction was caused by non-virion-associated CD63, we pretreated HIV-1 particles or target cells with the culture supernatant of the cells transfected solely with pCD63 (Fig. 3A) and evaluated the effect on HIV-1 infectivity by Magi assay. However, non-virion-associated CD63 did not affect HIV-1 infectivity (Fig. 3B to D). Moreover, we also examined whether non-virion-associated CD63 interferes with the virus precipitation assay. As shown in Fig. 3E, however, non-virion-associated CD63 did not affect virus precipitation by anti-

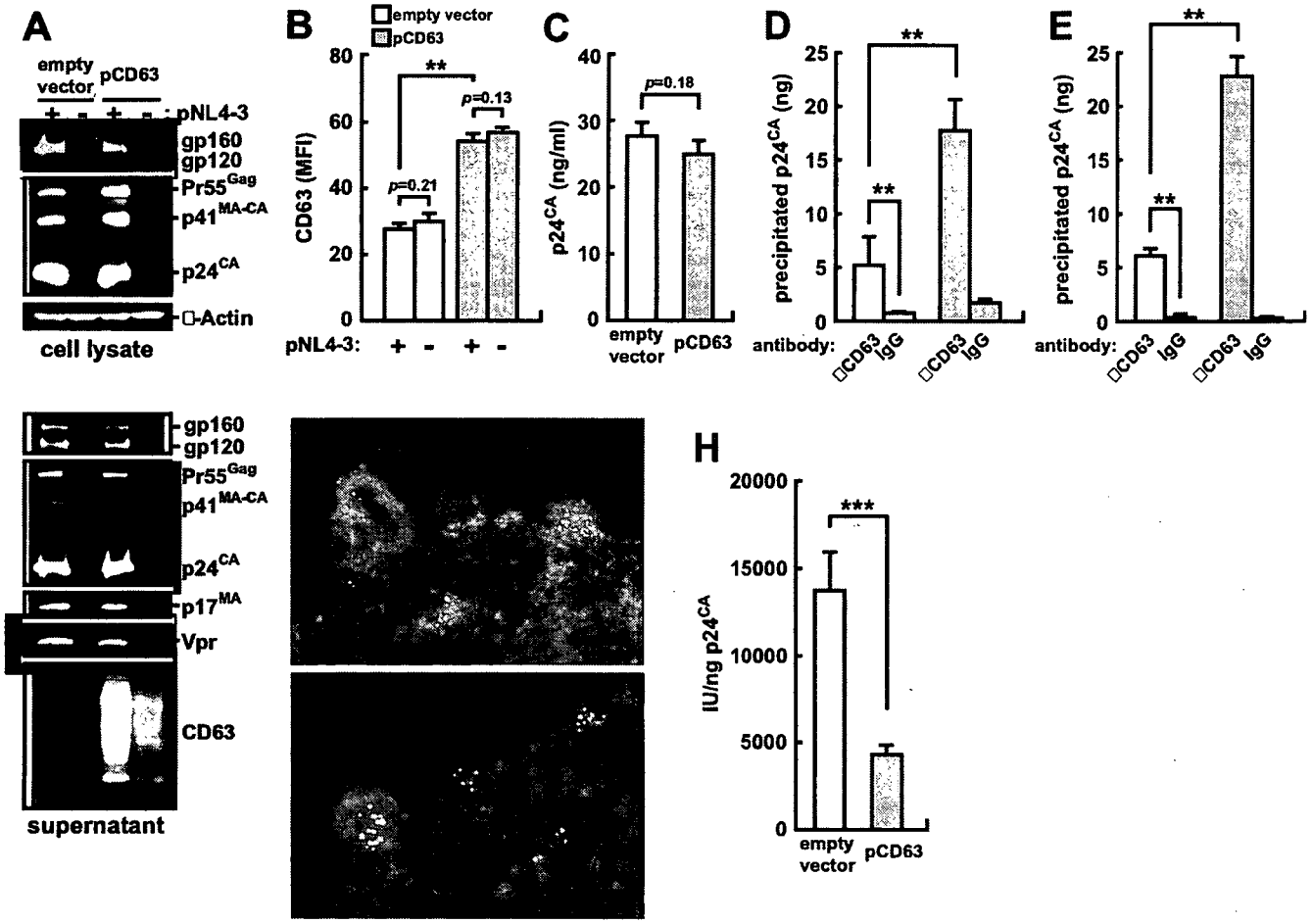

FIG. 2. Incorporation of exogenous CD63 into released HIV-1 virions and suppression of infectivity. Plasmid DNAs (pNL4-3 and either pCD63 or empty vector) were cotransfected into 293T cells as described in Materials and Methods. (A) Viral protein expression in the transfected 293T cells (cell lysate) and viral components in released HIV-1_{NL4-3} particles (supernatant) were analyzed by Western blotting, and a representative result is shown. The cell number was normalized to -actin, and the released virions were harvested as described in Materials and Methods. (B) The surface expression of CD63 on empty vector-cotransfected and pCD63-cotransfected 293T cells was analyzed by flow cytometry. (C) The amount of released HIV-1_{NL4-3} particles released from empty vector-cotransfected or pCD63-cotransfected 293T cells was quantitated by $p24^{CA}$ ELISA. (D and E) HIV-1_{NL4-3} particles (D) and virus-like particles (E) (100 ng of $p24^{CA}$) released from empty vector-cotransfected or pCD63-cotransfected 293T cells were used for immunoprecipitation by respective antibodies, and the assay was performed as described in Materials and Methods. (F and G) Immunoelectron microscopy was performed as described in Materials and Methods. CD63 on HIV-1_{NL4-3} particles released from empty vector-cotransfected (F) and pCD63-cotransfected (G) 293T cells was detected by using anti-CD63 mouse antibody and was visualized with anti-mouse IgG 5-nm gold colloid (black dots). Bars, 100 nm. (H) IU of HIV-1_{NL4-3} released from empty vector-cotransfected or pCD63-cotransfected 293T cells were measured by Magi assay and were normalized to $p24^{CA}$. Experiments were performed in triplicate. Statistical significance (Student's *t* test) is shown as follows: **, P 0.01; ***, P 0.001. Error bars indicate standard deviations. MFI, mean fluorescence intensity.

CD63 antibody. In summary, the data suggest that only CD63 proteins incorporated into released virions have a role in the attenuation of HIV-1 infectivity.

CD63 on the cell surface is preferentially incorporated into the released virions. To investigate the correlation between HIV-1 infectivity and the level of CD63 on the released virions and on the surfaces of HIV-1-producing cells, we prepared pCD63 L, expressing a lysosomal target motif-deleted CD63. In agreement with a previous report (34), CD63 L was present in larger quantities on the cell surface than wild-type CD63 was (Fig. 4B), although the total amount of expressed protein was comparable to that of wild-type CD63 (Fig. 4A, top).

Using this plasmid, we investigated the effect of CD63 L on the infectivity of released virions. Although CD63 L did not affect the amount of either $p24^{CA}$ or gp120 released into the culture supernatant (Fig. 4A and C), it severely attenuated the infectivity of released NL4-3 (Fig. 4D). Furthermore, we noticed that CD63 L was incorporated into released virions in larger amounts than wild-type CD63 (Fig. 4E). These results suggest that infectivity is inversely correlated with the amount of CD63 (CD63 L) on both the released virions and the plasma membranes of HIV-1-producing cells.

Virion-incorporated CD63 impairs NL4-3 Env- and IIIB Env- but not JR-FL Env-mediated infection. To analyze the effect of virion-incorporated CD63 on other HIV-1 strains, we next cotransfected with pJR-FL and pCD63 into 293T cells. As in the case of NL4-3, exogenous CD63 did not affect the amount of released virions and was successfully incorporated

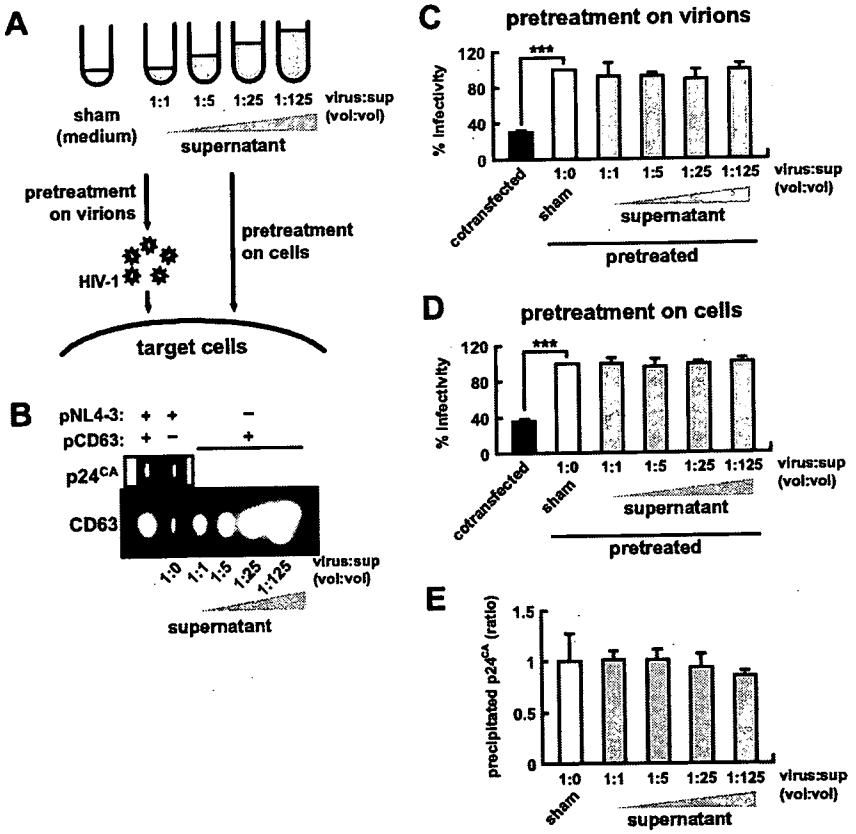

FIG. 3. Effect of non-virion-associated CD63. (A) Schematic diagram of the assay used for panels C and D. (B) Slot blotting shows the relative amounts of CD63 in each culture supernatant used for treatment. (C and D) Non-virion-associated CD63 was used to pretreat virions (C) or target cells (D), and the effect was assessed by Magi assay. RPMI 1640 was used as negative controls (sham), and the infectivity in controls was defined as 100%. The black bars indicate the infectivity of the virions released from the 293T cells cotransfected with pNL4-3 and pCD63, used as positive controls. (E) Effect of non-virion-associated CD63 in a virus precipitation assay. The amount of precipitated virions was quantified as described in Materials and Methods, and the ratio of amounts of precipitated virions to the sham-pretreated control was shown. The relative volumes of the supernatant shown schematically (A) and quantitatively (B) are identical to those used for panels C to E. Experiments were performed in triplicate. The *P* value versus sham-pretreated controls is 0.001 by Student's *t* test (***). Error bars indicate standard deviations.

into the released JR-FL (data not shown). However, virion-incorporated CD63 did not attenuate the infectivity of JR-FL (Fig. 5B).

NL4-3 uses CXCR4 as its coreceptor, whereas JR-FL uses CCR5, and coreceptor usage is severely dependent on the V3 region of Env (11). To investigate the possibility that the function of virion-incorporated CD63 is dependent on coreceptor usage, we used a chimeric HIV-1, NLFLV3. Although NLFLV3 uses CCR5 as its coreceptor (Fig. 5A) (18, 63), the infectivity of NLFLV3 was suppressed in a manner similar to that of wild-type NL4-3 (Fig. 5B). This result indicates that CD63 has the potential to reduce the infectivity of HIV-1 virions in a strain-specific manner and that it does not depend on coreceptor usage.

By cotransfecting pCD63 and pNLLuc, which has a defect in *env* and contains the luciferase gene (*luc*) in NL4-3 DNA, with Env (NL4-3 Env, IIIB Env, a CT-deleted NL4-3 [NL4-3 CT] Env, JR-FL Env, or VSV-G) expression plasmids, we prepared various pseudotyped viruses that each have Env on the *luc*-carrying particles. We observed that virion-incorporated CD63 suppressed the infectivity of viruses pseudotyped with NL4-3 Env (Fig. 6A) and IIIB Env (Fig. 6B) in a dose-dependent manner but did not affect that of viruses pseudotyped with JR-FL Env (Fig. 6D) and VSV-G (Fig. 6E). In addition, we found that the infectivity of viruses pseudotyped with NL4-3 CT Env was also attenuated through exogenous CD63 (Fig. 6C). Although it has been reported that the impediment of the association between Env CT and $p17^{MA}$ leads to repression of HIV-1 infection (16, 73), this result indicates that virion-incorporated CD63 does not affect the association of Env CT and $p17^{MA}$ at the lining of the viral membrane. Since the pseudotyped viruses differ only in Env, these results indicate that the effect of virion-incorporated CD63 is determined by Env. Moreover, the reduction in infectivity was also confirmed in activated primary CD4 T cells (Fig. 6F).

Virion-incorporated CD63 inhibits HIV-1 infection at the postattachment entry step(s). The process of HIV-1 entry into target cells has been extensively studied (23). The results described above indicate that virion-incorporated CD63 has the potential to disrupt NL4-3 and IIIB Env-mediated virus entry, and the disruption can negatively influence either attachment to CD4 on target cells or a conformational change of Env leading to virus-to-cell fusion mediated by gp41.

To address these possibilities, we initially compared the